The effect of four lanthanides onto a rat kidney cell line (NRK-52E) is dependent on the composition of the cell culture medium

Heller, A.; Pisarevskaja, A.; Bölicke, N.; Barkleit, A.; Bok, F.; Wober, J.;

Originally published:

May 2021

Toxicology 456(2021), 152771

DOI: https://doi.org/10.1016/j.tox.2021.152771

Perma-Link to Publication Repository of HZDR:

https://www.hzdr.de/publications/Publ-31698

The effect of four lanthanides onto a rat kidney cell line (NRK-52E) is dependent on the composition of the cell culture medium

Anne Heller[a‡], Alina Pisarevskaja[a], Nora Bölicke[a], Astrid Barkleit[b], Frank Bok[b], Jannette Wober[a]

[a] Technische Universität Dresden, School of Science, Faculty of Biology, Institute of Zoology, Chair of Molecular Cell Physiology and Endocrinology, Zellescher Weg 20b, 01217 Dresden, Germany

[b] Helmholtz-Zentrum Dresden-Rossendorf, Institute of Resource Ecology, Bautzner Landstraße 400, 01328 Dresden, Germany

‡ corresponding author; current address: Technische Universität Dresden, School of Science, Faculty of Chemistry and Food Chemistry, Analytical Chemistry, Chair of Radiochemistry/Radioecology, Zellescher Weg 19, 01069 Dresden, Germany

E-mail addresses:

anne.heller@tu-dresden.de

alina.pisarevskaja@tu-dresden.de

nora.boelicke@tu-dresden.de

a.barkleit@hzdr.de

f.bok@hzdr.de

jannette.wober@tu-dresden.de

Abstract

Lanthanide (Ln) exposure poses a serious health risk to animals and humans. In this study, we investigated the effect of 10^{-9} - 10^{-3} M La, Ce, Eu, and Yb exposure onto the viability of rat renal NRK-52E cells in dependence on Ln concentration, exposure time, and composition of the cell culture medium. Especially, the influence of fetal bovine serum (FBS) and citrate onto Ln cytotoxicity, solubility, and speciation was investigated. For this, *in vitro* cell viability studies using the XTT assay and fluorescence microscopic investigations were combined with solubility and speciation studies using TRLFS and ICP-MS, respectively. The theoretical Ln speciation was predicted using thermodynamic modeling.

All Ln exhibit a concentration- and time-dependent effect on NRK-52E cells. FBS is the key parameter influencing both Ln solubility and cytotoxicity. We demonstrate that FBS is able to bind Ln^{3+} ions, thus, promoting solubility and reducing cytotoxicity after Ln exposure for 24 and 48 h. In contrast, citrate addition to the cell culture medium has no significant effect on Ln solubility and speciation nor cytotoxicity after Ln exposure for 24 and 48 h. However, a striking increase of cell viability is observable after Ln exposure for 8 h. Out of the four Ln elements under investigation, Ce is the most effective.

Results from TRLFS and solubility measurements correlate well to those from *in vitro* cell culture experiments. In contrast, results from thermodynamic modeling do not correlate to TRLFS results, hence, demonstrating that big gaps in the database render this method, currently, inapplicable for the prediction of Ln speciation in cell culture media. Finally, this study demonstrates the importance and the synergistic effects of combining chemical and spectroscopic methods with cell culture techniques and biological methods.

Keywords: f-elements; speciation; cytotoxicity; XTT; time-resolved laser-induced fluorescence spectroscopy; thermodynamic modeling

Highlights:

- Ln cytotoxicity depends on Ln concentration, exposure time, and medium composition.
- At environmental concentrations, Ln exhibit no harmful effect within 8 – 48 h.
- At elevated concentrations, Ce has the potential to harmfully affect kidney cells.
- FBS has a greater influence on Ln cytotoxicity, solubility, speciation than citrate.
- In citrate medium, 8 h exposure with Ce lead to significantly enhanced cell viability.

1. Introduction

Lanthanides (Ln) are counted among the emerging pollutants (Gwenzi et al., 2018; Tepe et al., 2014), since recently the increased demand has led to a substantial increase in mining and processing activities worldwide, especially in China. Consequently, this leads to an elevated release of Ln into the environment. Ln have unique properties making them valuable for a wide range of industrial, medical, agricultural, and even zoo-technical applications. Amongst others they are contained in smart phones, fiber optics, flat screens, permanent magnets, batteries, contrast agents for magnetic resonance imaging, phosphate binders in medicine, fertilizers, and food additives (Aquilina et al., 2016; Gwenzi et al., 2018; Harrison and Scott, 2004; Hirano and Suzuki, 1996; Hu et al., 2004; Pagano et al., 2015; Rim et al., 2013; Wells and Wells, 2012).

Once released, Ln are spread in the environment with ground and surface water. They are reported to accumulate in vegetation, invertebrates, and vertebrates (Durbin, 1960; Durbin, 1962; MacMillan et al., 2017) as well as humans (Leggett et al., 2014). Human exposure to Ln can occur through various routes alongside the whole value creation chain by inhalation, ingestion, and wounds. Today, ingestion of contaminated food and drinking water as well as direct uptake via medical administration or occupational exposure are considered to be the main transfer routes for Ln from the environment into the human organism (Gwenzi et al., 2018).

Natural concentrations for unexposed rivers and mineral waters in China, Germany, and the USA are reported to be ≤ 9 µg/l for the sum of all Ln (Hatje et al., 2016; Kulaksiz and Bau, 2013; Li et al., 2014; Moeller et al., 2014; Negrel et al., 2000; Tepe et al., 2014; Zhang et al., 2000). For a single element, natural concentrations vary widely, e. g. between 1.2 and 170 ng/L in the case of Ce (Kulaksiz and Bau, 2013). However, studies

conducted in Ln mining areas of China, report Ln concentrations in exposed rivers and tap water that are much higher (He et al., 2010; Zhang et al., 2000). That is, e. g. in a tributary to the Yellow River, the sum of all Ln is reported to amount to 8,500 µg/L and the Ce concentration is 3,380 µg/L (He et al., 2010). For this tributary, the Ce concentration is at least four magnitudes higher than in unexposed natural waters.

The same is evident for blood samples of Chinese people living in exposed and control areas, respectively. Reported blood levels of unexposed control groups range from 0.97 to 4.07 µg/L for the sum of all Ln as well as from 0.01 to 0.66 µg/L for Ce (Li et al., 2013; Yu et al., 2007). In contrast, Ln sum concentration measured in the blood of people living in a mining area is reported to amount to 1,108 µg/L and the Ce concentration is reported to add up to 603 µg/L (Li et al., 2014; Li et al., 2013), which both are three magnitudes higher than the respective reference value. This illustrates a significant enrichment of Ln in body fluids.

After incorporation, Ln are absorbed into the blood stream and interact with its constituents, especially proteins (Leggett et al., 2014; Taylor, 1998). They are rapidly cleared from blood and redistributed to target organs and tissues all over the body (Höllriegl et al., 2020; Leggett et al., 2014). Excretion occurs mainly *via* the kidneys with urine (Durbin, 1960; Durbin, 1962; Höllriegl et al., 2017; Leggett et al., 2014). In rats, the urinary excretion peaks within the first three days and accumulates to 20 – 30 % of the injected Ln amount (Durbin, 1960; Durbin, 1962; Leggett et al., 2014). In humans, Ln excretion is very fast and peaks within 8 h to about 6 % of the injected Ln amount (Höllriegl et al., 2020; Höllriegl et al., 2017).

The current state of knowledge about the health effects of Ln in animals and humans is surveyed in several reviews (Gwenzi et al., 2018; Hirano and Suzuki, 1996; Leggett et al.,

2014; Pagano et al., 2015; Rim et al., 2013; Wells and Wells, 2012). Concerning animals, Ln are demonstrated to be toxic to rats and mice (Durbin, 1960; Durbin, 1962; Feng et al., 2007; Hirano and Suzuki, 1996; Nakamura et al., 1997; Zhao et al., 2013), dogs (Cuddihy and Boecker, 1970; Cuddihy and Griffith, 1971; Cuddihy and Griffith, 1972; Richmond and London, 1966), monkeys (Ducousso and Pasquier, 1974), sea urchins (Hirano and Suzuki, 1996; Oral et al., 2017; Pagano et al., 2015; Pagano et al., 2016; Trifuoggi et al., 2017), and aquatic midges (Kumar et al., 2016). In the case of humans, several adverse health effects are documented, amongst them severe damage to the nephrological system (Cheng et al., 2012; Fraum et al., 2017; Gwenzi et al., 2018; Hirano and Suzuki, 1996; Maulik et al., 1983; Spencer et al., 1997; Vergauwen et al., 2018), carcinogenesis (Rim et al., 2013), dysfunctional neurological disorder (Gwenzi et al., 2018; Zhu et al., 1996), tissue fibrosis (Gwenzi et al., 2018; Rim et al., 2013) as well as pneumoconiosis and interstitial lung disease (Pagano et al., 2015; Porru et al., 2001).

The kidneys are reported to bear the greatest initial Ln deposition of all soft tissues (Spencer et al., 1997) and the tubule seems to be the renal part which is affected the most. (Hirano and Suzuki, 1996) report a reduced urinary concentrating ability and an increased renal vascular resistance upon Ln exposure of rats. Mineral deposits in the glomerular and papillary capillaries of the kidneys of Ln exposed rats were reported by (Spencer et al., 1997) and associated with Ln toxicity. Furthermore, these authors detected multifocal necrosis of the proximal convoluted tubule. After long-term exposure of mice with low Ln doses, ambiguity of the renal architecture and congestion of renal blood vessels and capillaries leading to functional impairment of the kidneys are reported (Cheng et al., 2012). Another part affected by Ln exposure seems to be the renal cortex. Using Ln exposed chicken, (Maulik et al., 1983) found an alterated level of enzymes of the antioxidant defense system, especially enzymes of the cytochrome P450 family,

located in this part of the kidney. Finally, concerning Gadolinium-based contrast agents for magnetic resonance imaging, nephrogenic systemic fibrosis is reported to be a severe adverse effect associated with Ln cytotoxicity (Fraum et al., 2017). However, up to now, the cellular and molecular mechanisms behind all these effects are still poorly understood.

One possibility to fill this gap are *in vitro* cell culture studies. Concerning mammalian cells, a bank of publications is reported for Ln exposure and toxicity studies. A short summary is given in (Heller et al., 2019). Briefly, both beneficial and detrimental effects on the cells are reported since the dose-response relationships of Ln often exhibit biphasic trends (Gwenzi et al., 2018) which is also called hormesis (Pagano et al., 2015). Accordingly, at very low concentrations, Ln can promote the growth and survival of cells (Schmidlin et al., 2012; Zhang et al., 2009), whereas the majority of publications reports cytotoxic effects of Ln on a variety of mammalian cells (Bladen et al., 2013; Dai et al., 2002; Feyerabend et al., 2010; Heller et al., 2019; Kubota et al., 2000; Paiva et al., 2009; Shen et al., 2010; Shen et al., 2009a; Shen et al., 2009b; Su et al., 2009; Yu et al., 2007; Yu et al., 2005).

With regard to kidney cells, a number of publications reports on the toxicity of common heavy metals on various cell lines derived from different species. Exposure of renal cells to U is also well investigated (Carriere et al., 2004; Carriere et al., 2005a; Carriere et al., 2005b; Carriere et al., 2008; Carriere et al., 2006; Milgram et al., 2007; Prat et al., 2005; Thiebault et al., 2007). However, for Ln, there is a lack of studies with mammalian renal cells. Therefore, in a previous study, we reported first results for rat renal NRK-52E cells and human renal HEK-293 cells exposed to La, Ce, Eu, and Yb for 8, 24, and 48 h, respectively, and demonstrated effects of all four Ln onto the viability of both cell lines at concentrations above 10^{-4} M Ln (Heller et al., 2019). Furthermore, Ln speciation in the cell

culture medium was experimentally investigated by time-resolved laser-induced fluorescence spectroscopy (TRLFS) as well as predicted by thermodynamic modeling (Heller et al., 2019).

To accompany cell culture studies on heavy metals with chemical and spectroscopic investigations is particularly important, since the chemical speciation of an element is one key factor determining its bioavailability and effect/toxicity (Ansoborlo et al., 2006; Apostoli, 1999; Bresson et al., 2012; Bresson et al., 2013; Carriere et al., 2005b; El-Akl et al., 2015; Khan et al., 2017; Kiss and Odani, 2007; Levina et al., 2017). In *in vitro* cell culture studies, the speciation of a heavy metal is determined mainly by the composition of the cell culture medium.

For standard cell culture medium supplemented with 10 % fetal bovine serum (FBS), we reported complete Ln solubility up to 10^{-3} M and, hence, proposed good bioavailability for the cells (Heller et al., 2019). However, other studies using mammalian and human cells conducted experiments in serum-free (no FBS) or serum-reduced (1, 2, or 5 % FBS) cell culture medium leading to diverse results (Carriere et al., 2004; Carriere et al., 2005a; Carriere et al., 2005b; Carriere et al., 2008; Carriere et al., 2006; Dominguez et al., 2002; Filerman and Berliner, 1980; Haase et al., 2015; Lawal and Ellis, 2010; Lee et al., 2017; Milgram et al., 2007; Prat et al., 2005). Only some of these works also report on the solubility of the studied heavy metal(s) in the respective cell culture medium (Carriere et al., 2005a; Carriere et al., 2008; Filerman and Berliner, 1980; Sachs et al., 2015).

Under natural and physiological conditions, citrate is an ubiquitous bioligand in the environment as well as the body and the most important low molecular weight ligand in body fluids for most heavy metals (Berthon, 2002). The average citrate concentration in

blood is about 0.1 mM (Abbott, 1983; Durbin, 2006). Several studies report an effect of citrate on the cytotoxicity of heavy metals. In the case of uranium (U), citrate was found to increase the cytotoxicity onto rat renal NRK-52E cells as well as the intracellular accumulation of the actinide while it had no influence on the U speciation (Carriere et al., 2006). In the case of Zn, exposed pig kidney LLC-PK1 cells are reported to exhibit sign of cytotoxicity only when Zn is mixed with citrate buffer, but not when administered in deionized water or phosphate buffered solution (Sargazi et al., 2013). In contrast to this, U showed no cytotoxicity or intracellular accumulation in LLC-PK1 cells when applied in citrate containing medium (Mirto et al., 1999).

To examine this issue for Ln, in the present study, we investigated the influence of the serum content, i. e. the FBS concentration, in the cell culture medium as well as that of citrate addition on the following parameters: i) the Ln cytotoxicity to rat NRK-52E cells, ii) the Ln solubility in the respective cell culture medium, and iii) the Ln speciation in the different media. The NRK-52E cell line is of noncancerous origin and, therefore, a representative model for animal and human kidney cells of the proximal tubule epithelium (Carriere et al., 2004). The influence of the serum content was investigated using serum-reduced medium (sr-medium) with only 1 % FBS and serum-free medium (sf-medium) without any FBS supplementation in comparison with the previously used standard medium (st-medium) with 10 % FBS. The influence of citrate was investigated using standard medium supplemented with 0.1 mM citrate (st-cit-medium).

Viability of NRK-52E cells was determined in all culture media as a function of Ln concentration using the XTT test after Ln exposure for 24 and 48 h, respectively. Where indicated, also experiments with short-time exposure for 8 h were performed. La, Ce, Eu, and Yb were chosen as representatives of light, middle, and heavy Ln. Ln concentrations ranged from 10^{-9} to 10^{-3} M to cover environmentally relevant trace concentrations, con-

centrations measured in blood samples of exposed workers, and concentrations near the solubility limit where significant effects occur. Dose-response curves were determined and effective concentrations for the half maximum effect (EC_{50} values) were derived. Accompanying the cell culture studies, the Ln solubility and speciation in the different cell culture media was determined using analytical and luminescence spectroscopic techniques. The results of this study contribute to an improved risk assessment for Ln in humans as well as to a better understanding of their environmental fate in the eco-sphere.

2. Materials and methods

2.1. Cell culture

Normal rat kidney cells (NRK-52E; (De Larco and Todaro, 1978)) representing noncancerous epithelial cells of the proximal tubulus were purchased from the Deutsche Sammlung für Mikroorganismen und Zellkulturen (ACC No. 199; Germany). Cells were cultivated in 75 cm^2 cell culture flasks (CELLSTAR®, greiner bio-one, Germany) in Dulbecco's Modified Eagle's Medium (DMEM; D5671; Sigma-Aldrich Chemie GmbH, Germany) supplemented with 10 % (v/v) fetal bovine serum (FBS; Capricorn Scientific GmbH, Germany), 4 mM glutamine and 1 % (v/v) penicillin/streptomycin (both purchased from Biowest, France) at 37 °C, 95 % relative humidity (rH), and 5 % CO_2. This medium is defined and referred to as "standard medium" (st). Cells were cultivated until confluence and passages 5 to 12 were used. Experiments were performed in cell culture media of various compositions (see Table 1): serum-reduced medium containing 1 % FBS (sr), serum-free medium without FBS (sf), and standard medium with additionally 0.1 mM citrate (st-cit).

Table 1: Composition of the cell culture media used within this study.

medium (abbreviation)	FBS content (v/v %)	citrate content (mM)	other supplements[a]
standard (st)	10	0	1 % Pen/Strep 4 mM Gln
serum-reduced (sr)	1	0	1 % Pen/Strep 4 mM Gln
serum-free (sf)	0	0	1 % Pen/Strep 4 mM Gln
citrate-containing (st-cit)	10	0.1	1 % Pen/Strep 4 mM Gln

[a] … basic medium is high glucose DMEM (see text).

2.2. Chemicals

La, Ce, Eu, and Yb were applied as chlorides or as their citrates. In the first case, stock solutions of 10^{-2} M Ln chlorides ($LnCl_3 \cdot 6$ or $7\ H_2O$, ≥ 99.9 % trace metal basis; Sigma-Aldrich Chemie GmbH, Germany) were prepared. For the latter case, a stock solution of 0.1 mM citrate was prepared by dissolving tri-sodium citrate dihydrate ($C_6H_5Na_3O_7 \cdot 2H_2O$, ≥ 99 %, p.a., ACS; Carl Roth GmbH + Co. KG, Germany). All stock solutions were prepared in double distilled, sterile water and stored at room temperature. In the case Ln stock solutions turned turbid, they were filtered through 0.45 µm sterile filters (Whatman®, GE Healthcare Life Sciences, Germany). Ln citrate solutions were, then, prepared directly within the cell culture experiments prior to adding medium to the samples.

As reported previously (Heller et al., 2019), $ZnCl_2$ (z. A.; Merck KGaA, Germany) was used as the positive control for XTT measurements, since it is reported to be cytotoxic to rat renal NRK-52E cells as well as pig renal LLC-PK1 cells (Milgram et al., 2007; Sargazi et al., 2013). A Zn stock solution of 10^{-2} M was prepared in double distilled, sterile water and stored at room temperature. The concentration of all Ln and Zn stock solutions was

verified by mass spectrometry with inductively coupled plasma (ICP-MS). For ICP-MS parameters see section 2.5.

The pH of the citrate stock solution was measured and adjusted to pH 7.4 ± 0.1 using HCl and/or NaOH. In case of the Ln and Zn, a pH > 7 leads to precipitation of hydroxides and carbonates. Therefore, heavy metal stock solutions were adjusted to pH 6.5 ± 0.2. Working solutions have, then, been prepared by dilution of the stock solutions with double distilled, sterile water.

For cell culture experiments, the following solutions and reagents were prepared and stored at -20 °C: i) 50 mg/mL XTT (2,3-Bis-(2-Methoxy-4-Nitro-5-Sulfophenyl)-2H-Tetrazolium-5-Carboxanilide) in DMEM, ii) 3 mg/mL PMS (5-Methylphenazinium methyl sulfate; both purchased from SERVA Electrophoresis GmbH, Germany) in phosphate buffered solution (PBS), iii) Phalloidin-iFluor™ 488 Conjugate (AAT Bioquest Inc., USA) in DMSO according to the manufacturer's protocol, iv) 5 mg/mL DAPI (4′,6-Diamidin-2-phenylindol; Santa Cruz Biotechnology Inc., USA) in water, v) 4 % (v/v) paraformaldehyde (96 %; Acros Organics, Belgium) in PBS, vi) 10 % (v/v) Triton X-100 (Sigma-Aldrich Chemie GmbH, Germany) in PBS, vii) 1 % (v/v) bovine serum albumin (BSA; AppliChem GmbH, Germany) in PBS, and viii) Mowiol 4-88 (Carl Roth GmbH + Co. KG, Germany) according to the manufacturer's protocol.

2.3. Determination of cell viability after Ln exposure

Details on the method were previously reported (Heller et al., 2019). Briefly, cells were sub-cultured in st-medium. For experiments in st-cit-medium, the cells grown in st-medium were directly used. For experiments in sr-medium, the cells were adapted to that medium one day prior to seeding into well plates, since the alteration of the serum content might have a significant effect on the cell metabolism interfering with the effect

of heavy metals. For this, st-medium was removed from the cell culture flask, the cells were washed with PBS and sr-medium was added. Then, the cells were incubated again for 24 h to adapt to these conditions.

For experiments, the cells were seeded in 96-well cell culture test plates (TPP Techno Plastic Products AG, Switzerland) at a density of $(4 – 6) \cdot 10^4$ cells/mL and incubated for 24 h to adhere to the plate surface. Then, the cell culture medium was removed, 100 µL of the respective fresh medium containing 10^{-9} – 10^{-3} M Ln as chloride or citrate was added and the sub-confluent cells were incubated again for 24 and 48 h, respectively. The pH of the respective medium was checked to be 7.6 ± 0.2 after addition of the highest Ln amount (compared to 7.8 ± 0.2 before Ln addition).

Viability of the exposed cells was measured using the XTT test (Scudiero et al., 1988). This test is based on the mitochondrial activity of the cells and measures the PMS mediated reduction of XTT to its colored formazan derivate, which can be monitored using a microplate reader (infinite F200, TECAN Trading AG, Switzerland) at 492 nm. The detailed experimental procedure is given in (Heller et al., 2019). As a negative control, untreated cells in sr- and st-cit-medium were used. In the case of st-cit-medium, another negative control of untreated cells in st-medium was also included to check whether citrate has any effect on the cell growth. As a positive control, cells exposed to $5 \cdot 10^{-4}$ M Zn were used, since this concentration was deduced from literature (Haase et al., 2015) and found to exhibit nearly complete cytotoxicity (see section 3.1, table 2 and section 3.2, table 3). For each Ln, studies were performed as three to six independent experiments with all blanks, controls, and samples at least in quadruplicates. Cell viability was, then, calculated in comparison to the negative control (equals 100 %) of each plate.

2.4. Cytochemical staining and microscopy

For cytochemical staining, cells in st-, sr- and st-cit-medium were seeded on glass slides equipped with a 8-well FlexiPerm (SARSTEDT AG & Co. KG, Germany) at a density of $4 \cdot 10^4$ cells/mL and incubated for 24 h to adhere to the glass surface. The subsequent exposure procedure was analog to the cell viability studies (see section 2.3).

The detailed experimental staining procedure is given in (Heller et al., 2019). In brief, cells were fixed on the glass slides with 4 % (v/v) paraformaldehyde, permeabilized with 0.1 % Triton X-100 and stained with Phalloidin in 1 % BSA. Then, they were embedded with cover slides and DAPI containing Mowiol. Finally, cells were left to dry overnight in the dark at room temperature and stored at 4 °C. In each plate, two wells remained untreated (negative control), two were treated with $5 \cdot 10^{-4}$ M Zn (positive control), and each two wells were exposed to 10^{-5} and 10^{-3} M Ce and Eu, respectively.

Fluorescence microscopy was performed on an Axio Vert.A1 equipped with an Axiocam 503 mono (both Carl Zeiss Microscopy GmbH, Germany) using LD A-Plan 20x/0.35 Ph 1 and 40x/0.55 Ph 1 objectives. For visualization of the stained cytoskeleton and nucleus, the GFP and DAPI fluorescence channels were used, respectively. For each channel, separate pictures with pseudo-color were taken and, then, an overlay was constructed using the ZEN 3.0 (blue edition) software (Carl Zeiss Microscopy GmbH, Germany).

2.5. Ln solubility in cell culture medium

The solubility of Ln in sr-, sf-, and st-cit-medium was determined for Ce, Eu, and Yb in 24-well cell culture test plates (TPP Techno Plastic Products AG, Switzerland) according to a method previously published (Heller et al., 2019). In each well, 2 mL of the respective cell culture medium containing 10^{-7} – 10^{-3} M Ln were incubated at 37 °C, 95 % rH,

and 5 % CO_2 for 24 and 48 h, respectively. In the case of st-cit-medium, again, Ln and citrate solutions were mixed prior to adding the st-medium. Afterwards, all samples were filtered through 0.45 µm sterile filters (Whatman®, GE Healthcare Life Sciences, Germany) and Ln concentrations in the filtrates were analyzed using ICP-MS. The measured Ln content represents the dissolved fraction of the applied total Ln concentration in the cell culture medium.

For cell culture medium with reduced Ln solubility, Ce and Eu were added to 30 mL of the respective medium to a final concentration of 10^{-3} M. Samples were incubated for 48 h and, afterwards, centrifuged for 5 min at 175 x g. The supernatant was discarded and the precipitate was analyzed with ICP-MS to determine the content of Ln, P, and Ca.

A second set of deposits was prepared in the same way, resuspended in bidestilled water and the total carbon (TC), total inorganic carbon (TIC), and total organic carbon (TOC) were analyzed. From these values, the carbonate content (as the sum of carbonate and hydrogen carbonate) of the deposits was calculated.

ICP-MS measurements were performed either on a NexION 350x (1300 W; Perkin Elmer, Germany) or an iCap RQ (1550 W; Thermo Fisher Scientific, Germany) each equipped with a quadrupole mass analyzer and argon as the plasma gas. Each measurement was performed in triplicates. TIC and TC measurement were performed on a "multi N/C 2100 S" (Analytik Jena, Germany). TIC was determined by passing the samples into phosphoric acid and blowing them off with oxygen. TC was measured by catalytic combustion of the samples in an oxygen stream at 800°C. For both methods, the formed carbon dioxide is measured using a nondispersive infrared sensor. The TOC, then, is the difference between TC and TIC.

2.6. Time-Resolved Laser-induced Fluorescence Spectroscopy (TRLFS)

Speciation studies of Eu in the different cell culture media were performed using a pulsed flash lamp pumped Nd:YAG-OPO laser system (Powerlite Precision II 9020 laser equipped with a Green PANTHER EX OPO; Continuum, USA) and an external delay generator (Model DG535; Stanford Research Systems, USA). Details on the experimental setup are reported in the literature (Moll et al., 2014). The laser pulse energy was 2.5 – 3.5 mJ and emission spectra were detected by an optical multichannel analyzer consisting of a monochromator and spectrograph (Andor Kymera SR328i; Oxford Instruments, UK) with different gratings (600 lines per mm were used) and an ICCD camera (Andor iStar DH320T-18U-63; Oxford Instruments Andor, UK). All experiments were performed at 200 µm slit width and 0.48 ms exposure time. All samples were maintained at T = 25 °C and, if precipitated, stirred using a qpod temperature-controlled sample compartment for fiber optic spectroscopy (Quantum Northwest, USA).

After excitation at 394 nm, steady-state and time-dependent luminescence spectra were recorded in the 570 – 640 nm range with delay times of 10 – 120 µs. Steady-state spectra exhibit three important luminescence peaks corresponding to the following emission transitions: i) $^5D_0 \rightarrow {}^7F_0$ at 575 – 580 nm, ii) $^5D_0 \rightarrow {}^7F_1$ at 585 – 600 nm, and iii) $^5D_0 \rightarrow {}^7F_2$ at 605 – 625 nm (Bünzli, 2010; Richardson, 1982). Since the $^7F_0$ peak results from a symmetry forbidden transition, it is very weak and occurs only in spectra of Eu complexes with asymmetrical first coordination shell. The $^7F_1$ peak results from a parity allowed magnetic dipole transition (MD) and its intensity should be hardly affected by complexation. Hence, it is used for normalization of the spectrum. In contrast, the $^7F_2$ peak results from a parity forbidden electric dipole transition (ED) and is strongly affected by complexation. Both the luminescence intensity and the fine structure of this peak are very sensitive to the ligand of the Eu^{3+} ion, which is why this transition is called

a hypersensitive transition (Bünzli, 2010; Richardson, 1982). Therefore, the intensity ratio of the ED over the MD transition ($R_{E/M}$; see section 2.8, equation 2) is an important parameter for comparing spectra of different Eu species. Luminescence decay curves of Eu can be mono or biexponential indicating the existence of one or two dominant binding forms.

2.7. Thermodynamic Modeling

The theoretical Ln speciation in sr-, sf-, and st-cit-medium (10^{-7} – 10^{-3} M, pH = 7.4, 5 % CO_2, T = 298.15 K) was predicted by thermodynamic modeling using the geochemical speciation code Geochemist's Workbench (GWB), Module React (vers. 12.0.2) (Bethke, 2008). The thermo.com.v8.r6+.dat database was used along with the accompanying code. The database was supplemented with current data for the aqueous complexation of Eu with various amino and organic acids (L-arginine, L-phenylalanine, L-tryptophan, L-valine and citric acid) as well as with their protolysis and complexation data with matrix ions (Ca, Mg, and Fe) taken from the JESS database (May et al., 2018). The thermodynamic data for transferrin complexation was included using Cm as a chemical analog (Bauer et al., 2014) as well as that for Eu complexation with bovine serum albumin (Li et al., 2007). Thermodynamic data of solid phases ($EuPO_4 \cdot 10\ H_2O$(s), $EuPO_4$(s), and $EuOHCO_3$(c) from HYDRA database (Puigdomènech, 2009)) were also included. If necessary, the thermodynamic stability or solubility constants have been recalculated to zero-ionic-strength conditions using the Davies equation (Davies, 1962). All thermodynamic data is given in the ESI, Table S1.

The composition of DMEM was taken from the supplier, the transferrin concentration in FBS was adopted from (Kakuta et al., 1997) and albumin concentrations from (Lindl, 2002). For transferrin, the reported value of 2 mg/mL (Heller et al., 2019) was assumed,

for albumin 0.75 mM. Consequently, 0.2 mg/mL transferrin and 0.075 mM albumin was used for all calculations in st-medium (10 % FBS) as well as 0.02 mg/L transferrin and 0.0075 mM albumin in sr-medium. For sf-medium, both proteins were omitted. In the case of st-cit-medium, the transferrin and albumin contents of st-medium were used and 0.1 mM citrate as well as the respective stability constants with Eu (Heller et al., 2012) included. Although various amino acids and other organic substances are present in DMEM and FBS, due to missing information about their concentrations (especially for FBS) and/or thermodynamic data for their interaction with Eu, they could not be taken into account for the modeling.

2.8. Data analysis and statistics

For cell viability studies, outlier detection using the Grubbs' test (Grubbs, 1969) was performed for each blank, control, and sample multiplicate. Then, dose-response curves were plotted using Origin (OriginPro 2015G, OriginLab Corporation, USA) and statistically evaluated for significances by one-way ANOVA with Tukey *post hoc* test ($p < 0.05$; 95 % confidence).

Cell viabilities were calculated in comparison to the negative control, i. e. untreated cells equal 100 %, and are given as means ± standard error of mean (SEM). Furthermore, the experimental dose-response curves of one Ln were fitted altogether in Origin using the following equation:

$$y = \frac{A_1 - A_2}{1 + \left(\frac{x}{x_0}\right)^p} + A_2 \,, \qquad (1)$$

where y is the cell viability after exposure to Ln, A_1 is the initial/highest cell viability, A_2 is the final/lowest cell viability, x is the Ln concentration, x_0 is the center of the curve,

and p is the power. A_2 is fixed to 0 %. Along with this fit, the EC_{50} ± SEM is calculated and equals x_0.

Luminescence spectroscopic data of Eu were also analyzed using Origin. First, all TRLFS spectra were baseline corrected and the steady-state spectra were normalized to the peak area of the $^5D_0 \rightarrow {}^7F_1$ band. Then, the $R_{E/M}$ was determined as follows:

$$R_{E/M} = \frac{I(^7F_2)}{I(^7F_1)}\,, \tag{2}$$

with I being the integrated luminescence intensity of the respective transition. Furthermore, Origin was used to determine the luminescence lifetime of emitting species according to the equation of exponential decay:

$$I(t) = \sum_i I_i \cdot e^{\left(\frac{t}{\tau_i}\right)}, \tag{3}$$

with I being the total luminescence intensity at the time t, I_i the luminescence intensity of species i at t = 0, and τ_i the corresponding luminescence lifetime. With this lifetime, the number of water molecules in the first coordination sphere (n_{H2O}) was calculated using the following equation (Kimura et al., 2001):

$$n_{H_2O} \pm 0.5 = \frac{1.05}{\tau} - 0.44\,. \tag{4}$$

In this empirical equation, the lifetime is inserted in ms. Using this number, the water molecules released from the inner coordination sphere of Eu(III) (Δn_{H2O}) were calculated according to (Ozaki et al., 2002):

$$\Delta n_{H_2O} \pm 0.5 = 9 - n_{H_2O}\,. \tag{5}$$

3. Results

This study covers *in vitro* cell culture experiments as well as cell free investigations. Using cell culture techniques, the effect of Ln onto the viability of rat renal NRK-52E cells in dependence on the composition of the cell culture medium was measured using the XTT test. Ln concentrations ranged from 10^{-9} to 10^{-3} M and exposure times were 24 and 48 h, respectively. When indicated, short-time measurements with 8 h exposure time were also performed. For each parameter set (Ln/exposure time/cell culture medium), dose-response curves were plotted and EC_{50} values derived. Furthermore, fluorescence microscopic studies were performed after cytochemical staining of NRK-52E cells. Cell free experiments comprised the determination of Ln solubility in the different cell culture media within the concentration range of 10^{-7} – 10^{-3} M as well as TRLFS investigations on and thermodynamic modeling of the Ln speciation, respectively. Experiments were carried out using La, Ce, Eu, and Yb under serum-reduced (sr; 1 % FBS), serum-free (sf; no FBS), and citrate-containing standard (st-cit; 10 % FBS + 0.1 mM citrate) conditions. Finally, the results are compared to previously published data obtained in standard cell culture medium (st; 10 % FBS) (Heller et al., 2019).

3.1. The influence of FBS on the solubility, cytotoxicity, and speciation of Ln

Ln solubility

Ln bind to a variety of ligands and form both soluble and insoluble complexes influencing the effect of Ln in cell culture experiments. Therefore, the solubility of Ce, Eu, and Yb in cell culture media of different FBS content was determined after incubation for 24 and 48 h using ICP-MS. Resulting solubility curves are depicted in Figure 1.

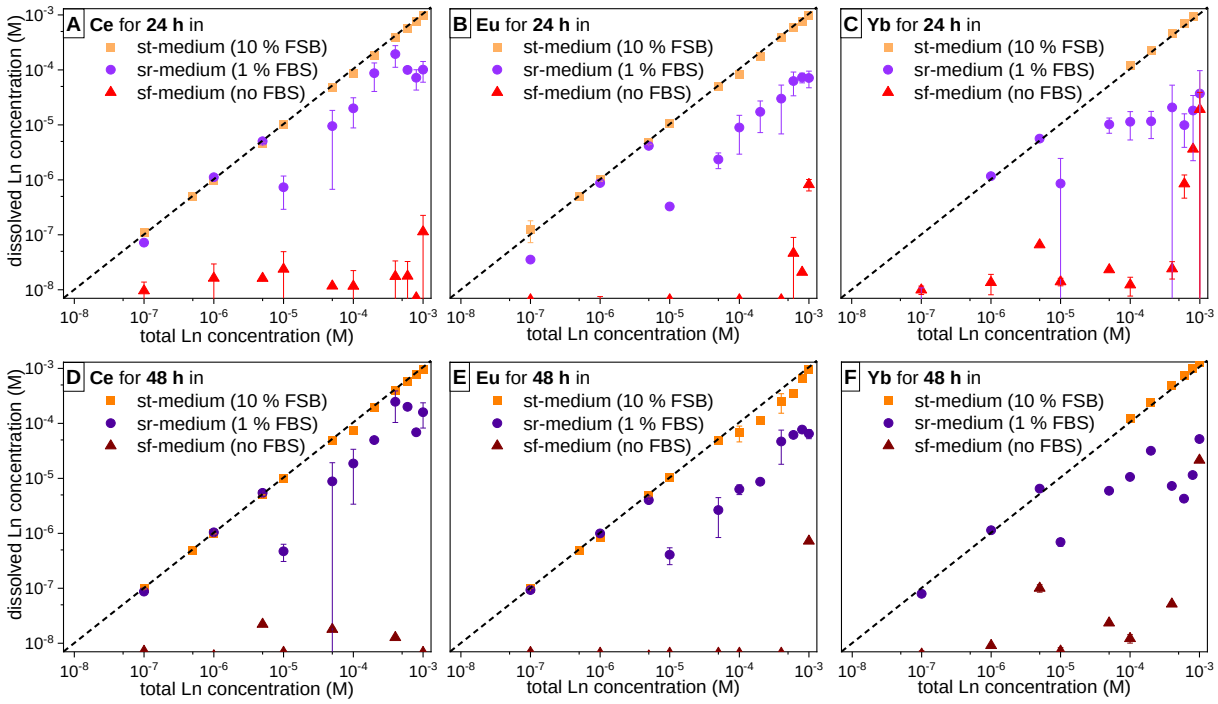

Figure 1: Solubility of Ce (A, D), Eu (B, E), and Yb (C, F) in cell culture media of different FBS content after incubation for 24 (A – C) and 48 h (D – F) as determined by ICP-MS. The dotted lines equal 100 % solubility. Values represent means ± SD of two to four independent experiments. Values below the limit of quantification (LOQ) were set to 1 µg/L (= LOQ). Data for st-medium were taken from (Heller et al., 2019).

In st-medium containing 10 % FBS, all three Ln are completely soluble up to 10^{-3} M. For sr-medium containing only 1 % FBS, this holds true for concentrations < 10^{-5} M Ln. At ≥ 10^{-5} M Ln, significant Ln precipitation occurs. White fluffy precipitates are visible by the eye at concentrations > $4 \cdot 10^{-4}$ M Ln. Furthermore, it seems like some kind of solubility plateau is reached at least for concentrations ≥ $4 \cdot 10^{-4}$ M Ln indicating saturated solutions. In sf-medium without any FBS supplementation, the solubility of all Ln is extremely low and the solutions seem to be saturated already at the lowest concentration of 10^{-7} M Ln. Hence, significant precipitation occurs which is visible as whitish jellylike deposits by the eye at least for > $2 \cdot 10^{-4}$ µM Ln. Both precipitations look different from each other.

The solubility curves of each Ln reveal no difference between the two incubation times in one respective medium. Hence, the solubility and potential precipitation seems to be

independent from time within our experiments. Furthermore, the solubility of all three elements is very similar in one respective cell culture medium. Therefore, the chemical behavior of all Ln can be considered as comparable and, hence, it is reasonable to assume that results for La would be similar.

Comparison between the three different cell culture media reveals that Ln solubility is increasing with increasing FBS content. This indicates Ln binding by constituents of FBS, most probably proteins, and is in accordance with previous investigations on Eu (Sachs et al., 2015) and Pb (Filerman and Berliner, 1980). Both of these studies report that FBS acts to solubilize or suspend the heavy metals in cell culture media.

In sr- and sf-medium, the known formation of poorly soluble Ln salts with phosphate, carbonate (both contained in DMEM), and hydroxide ions most probably is the cause for Ln precipitation. Using ICP-MS, we analyzed settled deposits of 10^{-3} M Ce and Eu in sr- and sf-medium, respectively, and found an elemental ratio for Ln : P of ~ 1 : 1 and for Ln : Ca of 1 : 0.2 in both cell culture media (see ESI, Table S2). This fits to the literature value of a settled and re-dissolved Eu precipitate from DMEM (Sachs et al., 2015). Hence, $LnPO_4$ seems to dominate the precipitated speciation. It is questionable whether precipitated Ln are bioavailable for the cells. The content of total organic (TOC) and inorganic carbon (TIC) of the deposits were also analyzed (see ESI, Table S2). Interestingly, TIC values are quite similar for each Ln in both sr- and sf-medium. Moreover, it is quite identical to the TIC of Ce and Eu deposits from DMEM alone (data not shown). In contrast, the TOC is almost three times higher in sr-medium than in sf-medium. The TOC values of the deposits from sf-medium are quite similar to those of deposits from DMEM alone (data not shown). This points, on the one hand, to different Ln deposits in sr- and sf-medium, respectively, confirming the observation that both precipitations have a differ-

ent appearance. On the other hand, this also indicates that, in sr-medium, in addition to phosphate, some component(s) of FBS might be involved in Ln precipitation.

In summary, our solubility data demonstrate that FBS is the key factor determining Ln solubility in cell culture media. Due to binding to (a) component(s) from FBS, most probably (a) protein(s), Ln are kept in solution. In contrast, without any FBS, Ln solubility is very low and Ln precipitate, most probably as phosphate species.

Ln impact onto NRK-52E cells in serum-reduced cell culture medium

The cell viability of NRK-52E cells in sr-medium was measured after exposure to La, Ce, Eu, and Yb for 24 and 48 h, respectively. Resulting dose-response curves are depicted in the ESI, Figure S1 and show a concentration-dependent effect for all Ln. All parameters are summarized in Table 2.

Prior to XTT measurements, the exposed cells were surveyed using a light microscope. In all wells with Ln concentrations ≥ $4 \cdot 10^{-4}$ M, precipitation was observed and masked the cells. For illustration, one picture of NRK-52E cells overlayed by Ln precipitation is given in the ESI, Figure S3. Along with this precipitation, we also observed increased values of the cell density measurement at 690 nm. Both observations correlate to the low solubility and precipitation of Ln in sr-medium.

After 24 h exposure, the cell viability is unaffected up to 10^{-5} M for all four elements. Higher Ln concentrations result in a gradual loss of cell viability. In the case of La and Yb, all alterations in cell viability were non-significant. The cell viability after exposure to 10^{-3} M Ln varies between 23.6 ± 7.0 % (Ce) and 73.9 ± 6.5 % (La). In the case of La, no EC_{50} value could be derived, since the fit of the dose-response curve failed. The EC_{50} values for the other Ln vary between $(1.8 \pm 0.4) \cdot 10^{-4}$ M (Ce) and $(1.1 \pm 0.2) \cdot 10^{-3}$ M (Eu).

After exposure for 48 h, dose-response-curves of all four Ln show an earlier onset of cell viability reduction. At 10^{-3} M Ln, the cell viability varies between 6.9 ± 1.8 % (Ce) and 31.7 ± 2.5 % (Eu). For all four Ln, EC_{50} values in the range of $(1.4 \pm 0.3) \cdot 10^{-5}$ M (Ce) and $(8.0 \pm 2.2) \cdot 10^{-4}$ M (Eu) were derived.

Since, except for Ce, no significant impact of Ln onto the viability of NRK-52E cells was observed after 24 h exposure, no short-time experiments were conducted in sr-medium.

Comparison of the cell viability at 10^{-3} M Ln in sr-medium with respect to the exposure times is depicted in the ESI, Figure S1C and dose-response curves of one respective Ln in dependence on the exposure time are given in the ESI, Figure S4A. Obviously, for each Ln, the cell viability at 10^{-3} M Ln is lower after 48 than after 24 h exposure. Hence, the impact of all four Ln onto NRK-52E cells seems to increase with prolonged exposure time. This is in accordance with the trend previously reported for st-medium (Heller et al., 2019) and also correlates to results from literature. (Dominguez et al., 2002) report the same time-dependence for the effect of Pb onto human fibroblasts in cell culture media with only 2 % FBS and (Carriere et al., 2004; Carriere et al., 2006) for the effect of U onto NRK-52E cells in sf-medium.

Comparison within the Ln yields the following toxicity gradient: Ce > La ~ Yb ~ Eu. Independent from the exposure time, Ce is the most effective element by far.

Serum-free experiments were not performed, since the NRK-52E cells were not able to cope with these conditions. After changing to sf-medium in the cell culture flask 24 h prior to seeding into 96-well plates, the cells started to die. Hence, negative controls did not grow properly, rendering the experiments unreliable.

Influence of FBS content on Ln cytotoxicity

The viability results of rat NRK-52E cells after exposure to Ln for 24 and 48 h in st- and sr-medium are compared with regard to the dose-response curves as well as to the cell viability at the highest Ln concentration. All data are summarized in Table 2 and Figure 2. Data in st-medium were taken from (Heller et al., 2019).

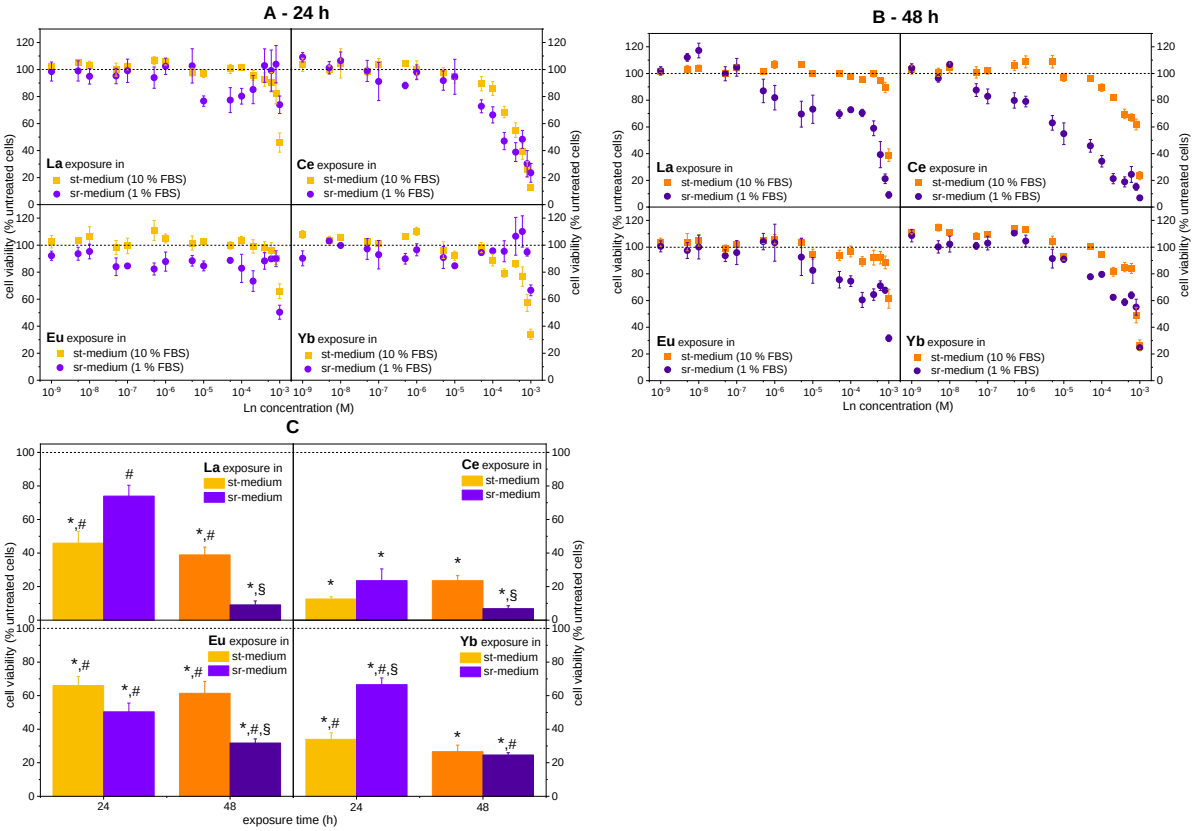

Figure 2: Comparative dose-response curves after Ln exposure of rat NRK-52E cells for 24 (A) and 48 h (B) in cell culture media of different FBS content as well as comparative cell viability ± SEM of rat NRK-52E cells after exposure to 1 mM Ln at the two exposure times (C; * = significant against untreated cells, # = significant against Ce, the most effective element, § = significant against standard cell culture medium). Values represent means of three to six independent experiments. Untreated cells equal 100 % cell viability (dotted lines). Significances are calculated with $p < 0.05$.

In general, after 24 h exposure, dose-response curves of one element show an analog trend in both cell culture media with cell viabilities being unaffected up to Ln concentrations of at least $5 \cdot 10^{-6}$ M and subsequent loss of cell viability at higher Ln concentrations (Figure 2A). In the case of Ce, dose-response curves are actually quite identical, whereas more or less significant differences can be seen for La, Eu, and Yb. Consequent-

ly, in both cell culture media the cell viability at the highest Ln concentration is very similar for Ce but differs for the other three Ln. Furthermore, independent from the FBS content, Ce exhibits a stronger effect onto NRK-52E cells than the other three Ln.

Table 2: Comparison of parameters derived from dose-response curves after Ln exposure of rat NRK-52E cells in cell culture media of different FBS content

metal	**medium**[a]	**24 h exposure cell viability at 10^{-3} M (%)**[b]	**EC_{50} value (µM)**[c]	**48 h exposure cell viability at 10^{-3} M (%)**[b]	**EC_{50} value (µM)**[c]
La	st[d]	46 ± 7	930 ± 25	39 ± 5	951 ± 10
	sr	74 ± 7	n. c.[e]	9 ± 2	304 ± 36
Ce	st[d]	13 ± 1	340 ± 29	24 ± 3	619 ± 25
	sr	24 ± 7	181 ± 37	7 ± 2	14 ± 3
Eu	st[d]	66 ± 5	1100 ± 39	61 ± 7	1070 ± 39
	sr	50 ± 5	1000 ± 170	32 ± 3	795 ± 220
Yb	st[d]	34 ± 4	790 ± 28	27 ± 4	779 ± 18
	sr	67 ± 4	1060 ± 85	25 ± 1	468 ± 44
Zn[e]	st[d]	3 ± 1	n. d.[f]	3 ± 2	n. d.[f]
	sr	0 ± 3	n. d.[f]	1 ± 1	n. d.[f]

[a] … st = standard medium (10 % FBS), sr = serum-reduced medium (1 % FBS)

[b] … values represent means ± SEM of three to eight independent experiments

[c] … values ± SEM derived from fitting of respective dose-response curves

[d] … (Heller et al., 2019)

[e] … positive control

[f] … n. d. = not determined

After 48 h exposure, dose-response curves of one element show an analog trend in both cell culture media (Figure 2B) but the impact onto NRK-52E cells is larger in sr-medium. This is especially evident for Ce, with the EC_{50} value in sr-medium being one magnitude lower than in st-medium. Again, in all cases, the lowest cell viabilities of NRK-52E cells were measured after exposure to Ce.

Comparison of both exposure times reveals that, in general, the effect of all Ln increases with prolonged exposure time in both cell culture media. Furthermore, obviously, the serum content of the medium plays a crucial role for the strength of Ln cytotoxicity. Reducing the FBS concentration from 10 to 1 % increases the cytotoxicity of all Ln after exposure for 48 h. This is especially evident for Ce. However, after 24 h exposure, dose-

response curves and EC_{50} values in sr-medium are quite similar to those in st-medium for all Ln.

The morphology of NRK-52E cells exposed to Ce in cell culture medium of different FBS content was studied via fluorescence microscopy after selective staining of the nucleus and the cytoskeleton. Reference pictures of untreated rat renal cells (negative control) in sr-medium are given in Figure 3A - C. In general, no significant morphological difference between control cells in st- and sr-medium is obvious (see ESI, Figure S5). Solely, the cell density might be a little bit lower in sr-medium. In both cell culture media, unexposed NRK-52E cells grow in a dense monolayer and exhibit a typical cobblestone shape with cell diameters of approximately 20 – 220 µm (mostly 30 – 80 µm). The cells are connected through close cell junctions and the cytochemical staining results in an intense fluorescence of nucleus and cytoskeleton. Furthermore, it is obvious that the cytoskeleton is much greater than the nucleus. Exposure to $5 \cdot 10^{-4}$ M Zn (positive control) leads to cell death and shrunken cells in both st- and sr-medium (see ESI, Figure S6). The cells look like small pinheads of approximately 10 – 20 µm diameter without any cell junctions and the cytoskeleton fluorescence is hardly obtained. Moreover, the cytoskeleton is nearly the size of the nucleus.

Fluorescence microscopic pictures of NRK-52E cells exposed to 10^{-3} M Ce for 48 h are depicted in Figure 3D – F. Again, observations are similar for both cell culture media. Hence, only pictures for sr-medium are presented. As can be clearly seen, part of the cells still exhibits the typical cobblestone shape of the untreated cells and forms a monolayer with quite close cell junctions. However, a significant part of the cells is shrunken and rounded, adopting a pinhead shape with cell diameters of approximately 15 – 40 µm. Cell junctions are loose or lost. The cytoskeleton is shrunken and significantly smaller than that of unexposed cells. Furthermore, the fluorescence intensity of the

Phalloidin staining is very low (yellow arrow). Partially, also nucleus condensation resulting in an enhanced intensity of the DAPI staining is observed (orange arrow).

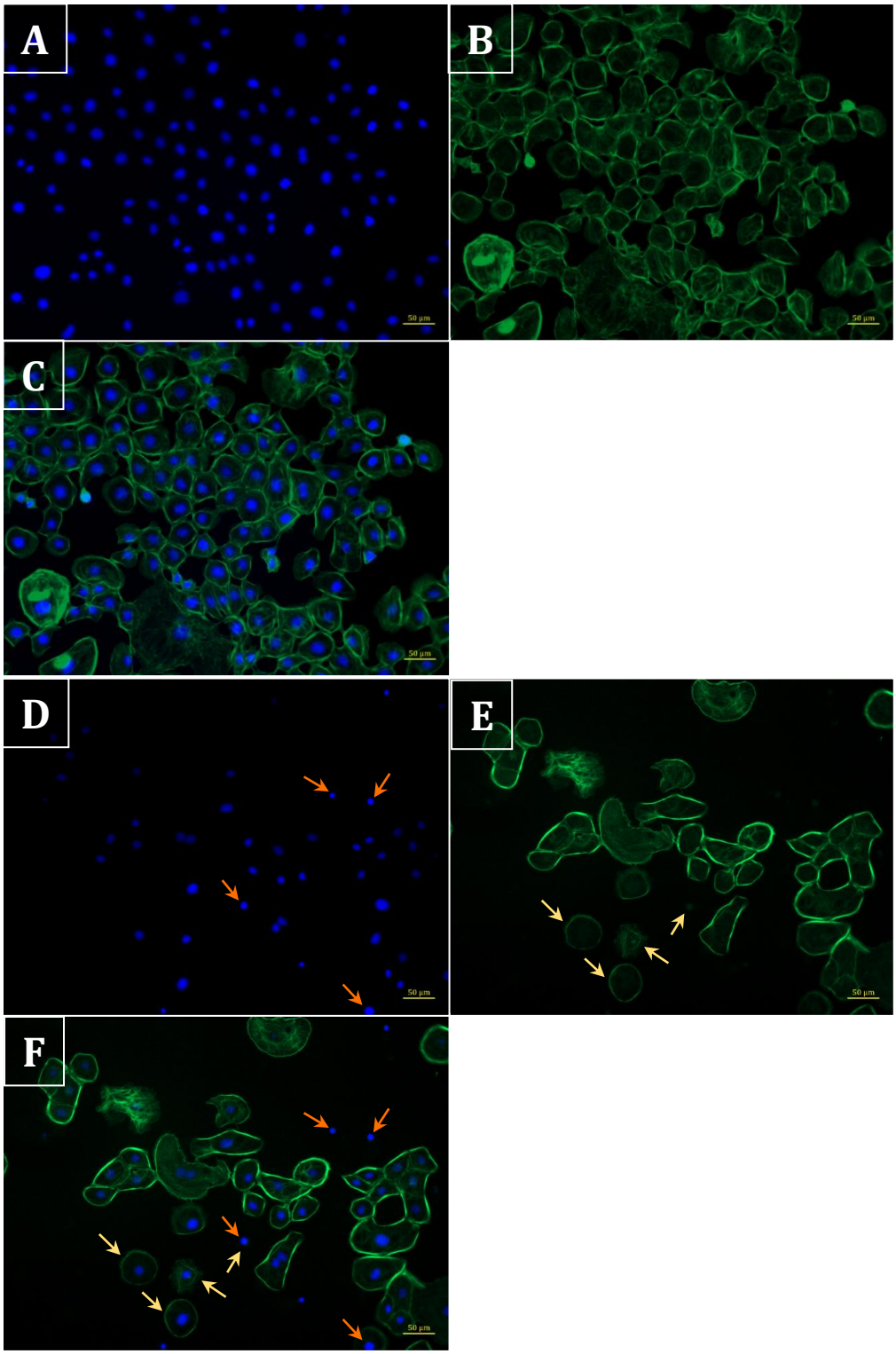

Figure 3: Fluorescence microscopic images of unexposed rat NRK-52E cells (A – C) and cells exposed to 10^{-3} M Ce for 48 h (D – F) both in sr-medium: (A, D) nucleus staining with DAPI, (B, E) cytoskeleton staining with Phalloidin, and (C, F) overlay of both stainings. The arrows indicate condensation of the nucleus (orange) as well as shrinking and/or loss of the cytoskeleton (yellow), respectively, upon Ce exposure. The bar represents 50 µm.

Comparing amplified fluorescence microscopic pictures of both untreated and Ce exposed cells illustrates the altered morphology (see ESI, Figure S7). In untreated cells, the fine structure of the cytoskeleton, i. e. a network of actin filaments and the cell membrane, are clearly visible. In contrast, within the cytoskeleton of Ce-exposed cells, holes can be observed. Actin filaments are not visible at all and, partially, also the cell membrane is not visible. In cases, where the cell membrane is still intact, the cytoskeleton is significantly shrunken. All these observations indicate cell death upon Ce exposure.

In summary, our cell culture results demonstrate that the strength of Ln cytotoxicity depends on the Ln concentration, the exposure time, and the FBS content of the medium. A lower FBS content strengthens the effect of Ln onto the viability of NRK-52E cells, at least after 48 h exposure. This is in accordance with the work of (Dominguez et al., 2002; Haase et al., 2015). After 24 h exposure, however, FBS has no significant effect on Ln cytotoxicity. Finally, for risk assessment derived from cell culture studies, it should be kept in mind, that proteins are ubiquitous in body fluids and that a serum content of 10 % FBS in cell culture medium equals about only 10 % of the physiological protein content *in vivo* (Haase et al., 2015).

Influence of FBS content on Ln speciation in cell culture medium

To get information about the Ln speciation, TRLFS studies in st-, sr-, and sf-medium were performed. Due to its striking luminescence properties, Eu was used in concentrations of 10^{-5} and 10^{-3} M, respectively, and steady-state as well as time-resolved luminescence spectra were recorded. To check, if the speciation changes within the time frame of the cell culture experiments, the samples were incubated for 24 and 48 h, respectively, in each medium prior to TRLFS. Results are depicted in the ESI, Figures S8 and S9. All spectral parameters are given in the ESI, Table S3.

Briefly, the following significant differences occur in comparison to the uncomplexed Eu^{3+} aqua ion: i) a small $^7F_0$ peak, ii) a splitting and great enhancement of the $^7F_2$ peak resulting in an inversed $R_{E/M}$, and iii) (very) long luminescence lifetimes. Both mono and biexponential luminescence decay occur in dependence on the cell culture medium and the Eu concentration.

In general, at constant Eu concentration, steady-state spectra and luminescence decay curves in one respective cell culture medium are very similar after incubation for 24 and 48 h, respectively. Hence, the Eu speciation in each medium remains unaltered within this time frame. This proves that the effects observed in the cell culture experiments are real time effects and not caused by a different Ln speciation.

Figure 4 depicts the steady-state spectra and luminescence decay curves in dependence on the FBS content of the cell culture medium.

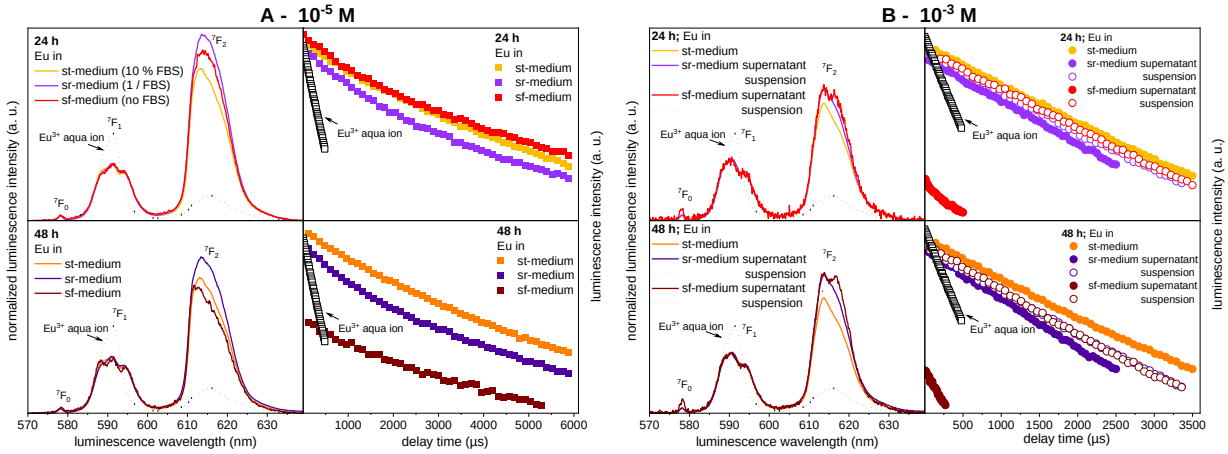

Figure 4: Comparative steady-state spectra and luminescence decay curves derived from time-resolved spectra of 10^{-5} M (A) and 10^{-3} M Eu (B) in cell culture media of different FBS content. Data of the Eu^{3+} aqua ion are given for comparison; luminescence bands are labeled with the respective ground state of the emission transitions. The luminescence spectra are scaled to the same height.

For 10^{-5} M Eu, spectra are very similar in all three cell culture media after incubation for 24 and 48 h, respectively (Figure 4A). Furthermore, also the spectral parameters are

very similar. The results indicate two coexisting Eu species with one to two and none water molecule(s) left in the inner sphere of the Eu^{3+} ion, respectively.

Raw data of the steady-state spectra (see ESI, Figure S10A) demonstrate that, at 10^{-5} M Eu, the luminescence intensity of Eu is highest in st-medium. In sr-medium, the luminescence intensity is about two third (24 h incubation time) or half (48 h incubation time) the maximum height and in sf-medium it is even one magnitude lower than in st-medium. This correlates to the solubility results and indicates that not all Eu is dissolved in those two cell culture media with the fraction of precipitated Eu being larger in sf- than in sr-medium. Since no precipitates were visible after centrifugation in both cell culture media, this might be an indication for colloidal Eu species. This hypothesis has to be proven by further investigations.

Using 10^{-3} M Eu, visible precipitation occurs in sr- and sf-medium. Hence, TRLFS spectra were recorded, on the one hand, in the supernatant after settlement of the precipitate and, on the other hand, in the stirred suspensions (Figure 4B). Additionally, the precipitated deposits were also measured (Figure 5 and ESI, Table S3). At constant incubation time, spectra and decay curves in st-medium, supernatant and suspension of sr-medium as well as the suspension of sf-medium are quite similar. Steady-state spectra and luminescence decay curves of the precipitated Eu deposits equal those in the respective cell culture medium suspension. The results indicate two coexisting Eu species with one and two water molecule(s) left in the inner sphere of the Eu^{3+} ion, respectively, in st-medium as well as one dominant Eu species with one to two water molecules in the coordination sphere in sr-medium and the suspension of sf-medium. In contrast, steady-spectra in the supernatant of the sf-medium are very different and the luminescence decay is significantly shorter. This indicates one dominant Eu species with six to seven water molecules left in the inner sphere of the Eu^{3+} ion.

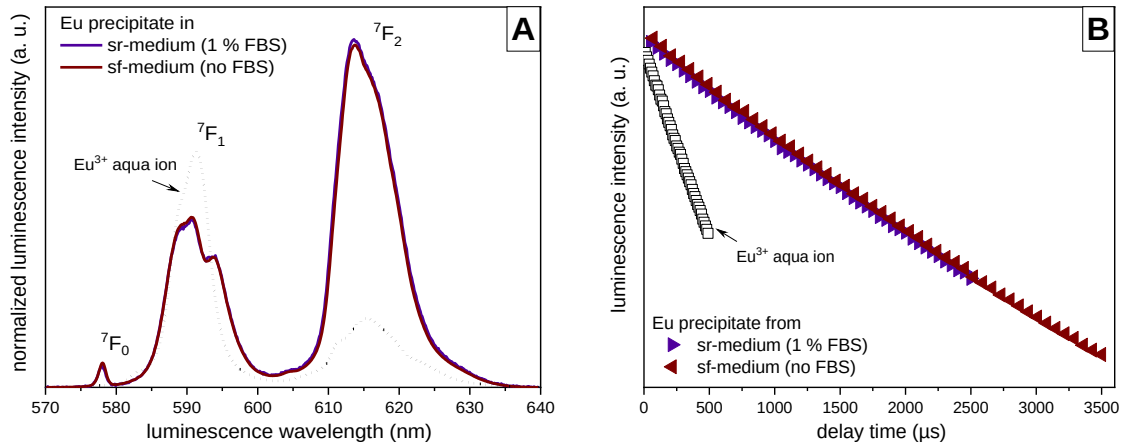

Figure 5: Steady-state luminescence spectra (A) and decay curves derived from time-resolved spectra (B) of precipitated deposits from sr- and sf-medium with 10^{-3} M Eu after 48 h incubation. Data of the Eu^{3+} aqua ion are given for comparison; luminescence bands are labeled with the respective ground state of the emission transitions. The luminescence spectra and decay curves, respectively, are scaled to the same height.

Raw data of the steady-state spectra (see ESI, Figure S10B) demonstrate that, at 10^{-3} M Eu, luminescence is highest in st-medium followed by sr-medium and lowest in sf-medium with the intensity being even two magnitudes lower. This reflects the solubility results and indicates that, in sf-medium, Eu is mostly precipitated and the Eu fraction remaining in solution is very small. In turn, in sr-medium, a larger Eu fraction is still in solution. With regard to the steady-state spectra and decay curves of the deposits from both cell culture media being nearly identical, it is reasonable to assume that the deposits precipitating from sr- and sf-medium contain the same dominant Eu species. Since sf-medium is without any FBS, this excludes proteins as ligands and points to inorganic anions, most probably phosphate and/or carbonate which are known to form hardly soluble Eu complexes. Again, this fits to the solubility results and elemental analysis data of the precipitated deposits which yielded an elemental ratio of Ln : P = 1 : 1. However, since luminescence curves of the deposit decay in a biexponential manner, this indicates a second Eu species within the deposits. With regard to the higher TOC in Ln deposits from sr-medium than from sf-medium (see ESI, Table S2), this might indicate that the minor Eu species in deposits from sr-medium contain (a) protein(s) from FBS, whereas

the minor Eu species in deposits from sf-medium has to be a protein-free species. This has to be further proven.

The remaining dissolved Eu fraction in sf-medium also has to be a protein-free species. Its short lifetime equaling six to seven water molecules still left in the first hydration shell of the Eu^{3+} ion indicates a complex with a small ligand. Hence, we assume a soluble Eu species most probably with an inorganic anion or with an organic low molecular weight ligand from DMEM (e. g. phosphate, carbonate, sulfate, nitrate, amino acids, or glucose).

Steady-state spectra of Eu in st-medium and sr-medium supernatant are also quite identical indicating the formation of the same Eu species. With regard to literature (Chen et al., 2001; Duffield et al., 1994; Palizban et al., 2010; Taylor, 1998) and previous investigations (Heller et al., 2019; Sachs et al., 2015), we suppose the formation of two soluble Eu complex species with proteins from FBS. Since proteins are big biomolecules replacing the majority or even all water molecules in the inner sphere of the Eu^{3+} ion upon complexation, this would account for the very long luminescence lifetimes. Furthermore, protein ligands geometrically distort the ligand sphere of the Eu^{3+} resulting in the observation of the forbidden $^7F_0$ peak as well as the great enhancement of the hypersensitive $^7F_2$ band. However, the actual nature of this/these species is yet unknown and has to be identified by ongoing, systematic TRLFS investigations using reference solutions of different composition and with transferrin as well as albumin as most promising candidates.

In summary, our TRLFS studies demonstrate that Ln speciation in one respective cell culture medium does not change within the time frame of 48h. Furthermore, TRLFS results correlate very well to those from Ln solubility studies. We suppose two soluble and

long-lived Eu species with proteins from FBS (Eu species 1 and 2) to be formed in st-medium. At least one of these species is also formed in sr-medium and remains in the supernatant after centrifugation. Furthermore, in sr-medium, a second, hardly soluble Eu species with inorganic anions from DMEM, most probably phosphate, (Eu species 3) is formed. The latter species also dominates the Eu speciation in sf-medium and the remaining Eu fraction in solution most probably is a soluble Eu species with an inorganic anion or an organic low molecular weight ligand from DMEM (Eu species 4). Hence, the FBS content has an influence not only on the solubility but also on the speciation of Eu in the cell culture medium. Once FBS is present, protein complexation dominates the Eu speciation and mediates its solubility in cell culture medium. Therefore, in the case of st- and sr-medium, we assume the same Eu species to dominate, whereas in sf-medium another Eu species clearly dominates. With regard to the cell culture experiments, this could explain why the effect of Ln onto NRK-52E is very similar in st- and sr-medium after exposure for 24 h. The stronger effect of Ln in sr- than in st-medium after 48 h exposure might be an indication that the amount of precipitated Eu is larger than after 24 h exposure.

Thermodynamic modeling of the Ln speciation in cell culture medium in dependence on the FBS content

To assist interpretation of the TRLFS data and to investigate the theoretical alterations of the Ln speciation in dependence on the FBS content, Eu speciation in sr- and sf-medium was predicted by thermodynamic modeling and compared to that reported for st-medium (Heller et al., 2019).

The predicted Eu speciation in sf-medium at both concentrations used for TRLFS is depicted in the ESI, Figure S11. At both 10^{-5} and 10^{-3} M Eu, in the experimental pH-range of

7.6 ± 0.2, the speciation is dominated by soluble carbonate and phosphate complexes with the negatively charged dicarbonato complex being the biggest fraction by far (> 70 %). Complexes with organic constituents are negligible. Strikingly, an identical Eu speciation is predicted in sr- and st-medium despite the serum content of 1 and 10 % FBS, respectively (data not shown). Only for 10^{-5} M Eu in st-medium, a very small fraction of Eu is calculated to exist as transferrin complexes at pH < 7.1 (Heller et al., 2019).

In summary, according to thermodynamic modeling, Eu speciation in st-, sr-, and sf-medium should be identical. Consequently, in st-, sr-, and sf-medium, also the TRLFS spectra and luminescence lifetimes should be identical. However, our TRLFS data demonstrate that this is not the case. Hence, it can be concluded that, currently, thermodynamic modeling cannot predict the effect of FBS on the Eu speciation in cell culture medium properly.

3.2. The influence of citrate on the solubility, cytotoxicity, and speciation of Ln

Ln solubility

The solubility of Ce, Eu, and Yb in cell culture media with and without citrate addition was determined after incubation for 24 and 48 h using ICP-MS after sterile filtration of the solutions. Resulting solubility curves are depicted in Figure 6.

All three Ln are completely soluble up to 10^{-3} M in both cell culture media. Furthermore, the solubility curves of each Ln reveal no difference between the two incubation times in one respective medium. Hence, Ln solubility seems to be independent from time within our experiments. Moreover, solubility of all three elements is quite identical in one respective medium. Therefore, the chemical behavior of all Ln can be considered as comparable and, hence, it is reasonable to assume that results for La would be similar.

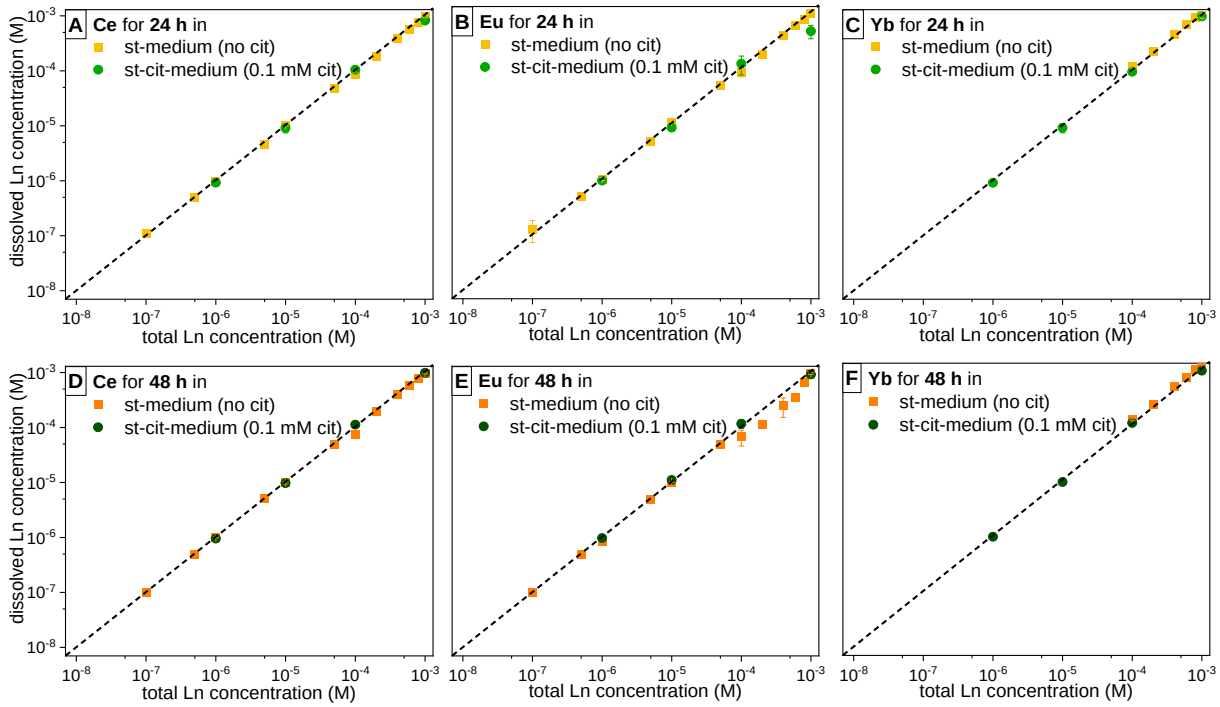

Figure 6: Solubility of Ce (A, D), Eu (B, E), and Yb (C, F) in standard cell culture media with and without citrate after incubation for 24 (A – C) and 48 h (D – F) as determined by ICP-MS. The dotted lines equal 100 % solubility. Values represent means ± SD of two to three independent experiments. Data for st-medium were taken from (Heller et al., 2019).

Comparison between both cell culture media reveals that the addition of citrate does not alter the solubility. This is in accordance with previous investigations on Eu (Sachs et al., 2015) as well as U (Carriere et al., 2006) and might be due to the fact that in both cell culture media the Ln are most probably complexed by serum proteins (Dominguez et al., 2002; Haase et al., 2015; Heller et al., 2019; Sachs et al., 2015; Sargazi et al., 2013). Citrate complexation is unlikely to be able to compete with this. Nevertheless, it is reasonable to assume that citrate complexation might compete with the formation of poorly soluble Ln salts with inorganic anions to a certain extent. This was demonstrated for Eu in sf-medium with and without citrate addition (Sachs et al., 2015). Hence, the potential of citrate to re-dissolve Ln in sr-medium should be further investigated in more detail.

Ln impact onto NRK-52E cells in citrate-containing cell culture medium

The cell viability of NRK-52E cells under citrate conditions was measured after exposure to La, Ce, Eu, and Yb for 8, 24 and 48 h, respectively. Resulting dose-response curves are depicted in the ESI, Figure S2 and show a concentration-dependent effect for all Ln. All parameters are summarized in Table 3.

To check whether citrate has any significant effect on the cell growth, a second negative control with untreated cells in st-medium without any citrate addition was included in each experiment. The cell viability of this control was measured to be 99 ± 5 %, 90 ± 3 %, and 94 ± 2 % after incubation for 8, 24, and 48 h compared to each 100 ± 12 % for the respective negative control in st-cit-medium. Hence, within 8 – 48 h, citrate addition in the culture medium has no significant effect on the growth of NRK-52E cells.

After 24 h exposure, the cell viability is unaffected up to $5 \cdot 10^{-6}$ M for all four elements. Higher Ln concentrations result in a gradual loss of cell viability. The cell viability after exposure to 10^{-3} M Ln varies between 20.8 ± 4.0 % (Ce) and 42.6 ± 2.0 % (Yb). From dose-response curves, EC_{50} values between $(2.6 \pm 0.6) \cdot 10^{-4}$ M (Ce) and $(7.3 \pm 0.8) \cdot 10^{-4}$ M (Yb) were calculated.

After exposure for 48 h, dose-response curves of all four Ln show a very similar progression. At 10^{-3} M Ln, the cell viabilities are quite comparable and lie in the range of 16.6 ± 4.0 % (Ce) and 24.6 ± 4.3 % (Eu). EC_{50} values range from $(6.8 \pm 0.3) \cdot 10^{-4}$ M (Ce) to $(8.5 \pm 0.3) \cdot 10^{-4}$ M (Eu).

Due to significant effects of all Ln after 24 h exposure, we also investigated short-time exposure for 8 h. As seen after 24 and 48 h, the Ln effect is concentration-dependent. Cell viability at 10^{-3} M Ln varies between 36.4 ± 3.7% (Ce) and 88.7 ± 10.7 % (La). EC_{50}

values range from $(1.1 \pm 0.3) \cdot 10^{-4}$ M (Ce) to $(6.4 \pm 1.6) \cdot 10^{-3}$ M Eu). Strikingly, at Ln concentrations < 10^{-5} M, the measured cell viability is > 100 %. This is especially evident for Ce and Yb. La and Eu show the same trend but to a lesser extent.

Comparison of the results in st-cit-medium with respect to the exposure time is depicted in the ESI, Figure S4B. For each Ln, the viability of NRK-52E cells is significantly lower after exposure for 24 and 48 h, respectively, than after short-time exposure for 8 h. No significant difference was observed between exposure for 24 and 48 h. Hence, the impact of all four Ln onto NRK-52E cells seems to increase with prolonged exposure time. This correlates to the trend previously reported for st-medium (Heller et al., 2019) and that observed in sr-medium (see section 3.1).

Comparison within the Ln yields the following toxicity gradient: Ce > La ≥ Yb ~ Eu. Notably, no significant difference can be determined between the effect of all four Ln after exposure for 48 h. In contrast, after exposure for 8 and 24 h, Ce is the most effective element.

Influence of citrate content on Ln cytotoxicity

The viability results of rat NRK-52E cells after exposure to Ln for 24 and 48 h in st- and st-cit-medium are compared with regard to the dose-response curves as well as to the cell viability at the highest Ln concentration. All data are summarized in Figure 7 and Table 3. Data in st-medium were taken from (Heller et al., 2019).

In general, after 24 h exposure, dose-response curves show an analog trend in both cell culture media with cell viabilities being unaffected up to Ln concentrations of at least $5 \cdot 10^{-6}$ M and subsequent loss of cell viability at higher Ln concentrations. In the case of Ce and Yb, dose-response curves are actually quite identical, whereas more or less

stronger effects in st-cit-medium can be seen for La and Eu. Consequently, the cell viability at the highest Ln concentration is very similar in both cell culture media for Ce and Yb, whereas it is lower in st-cit-medium for La and Eu. Nevertheless, independent from citrate addition, Ce exhibits a stronger effect onto NRK-52E cells than the other three Ln.

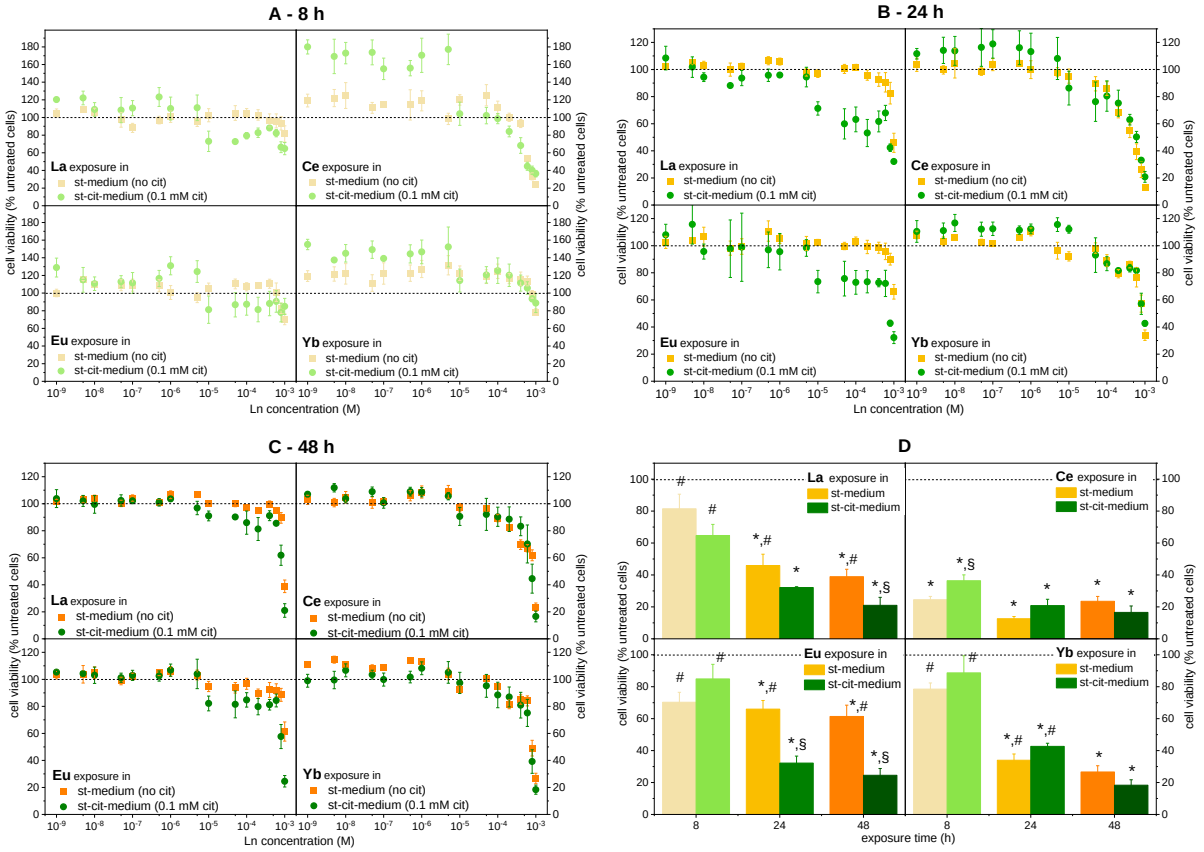

Figure 7: Comparative dose-response curves after Ln exposure of rat NRK-52E cells for 8 (A), 24 (B) and 48 h (C) in standard cell culture medium with and without citrate as well as comparative cell viability ± SEM of rat NRK-52E cells after exposure to 1 mM Ln at the three exposure times (D; * = significant against untreated cells, # = significant against Ce, the most effective element, § = significant against standard cell culture medium). Values represent means of three to six independent experiments. Untreated cells equal 100 % cell viability (dotted lines). Significances are calculated with $p < 0.05$.

After 48 h exposure, dose-response curves of one respective Ln are nearly identical in st- and st-cit-medium. Moreover, the EC_{50} values for one element are very similar and the cell viability at the highest Ln concentration is quite identical for Ce and Yb.

Table 3: Comparison of parameters derived from dose-response curves after Ln exposure of rat NRK-52E cells in cell culture media with and without citrate

Ln	medium[a]	8 h exposure cell viability at 10^{-3} M (%)[b]	EC_{50} value (µM)[c]	24 h exposure cell viability at 10^{-3} M (%)[b]	EC_{50} value (µM)[c]	48 h exposure cell viability at 10^{-3} M (%)[b]	EC_{50} value (µM)[c]
La	st[d]	81 ± 9	n. c.[e]	46 ± 7	930 ± 25	39 ± 5	951 ± 10
	st-cit	65 ± 7	592 ± 270	32 ± 1	349 ± 97	21 ± 5	828 ± 18
Ce	st[d]	25 ± 2	640 ± 32	13 ± 1	340 ±29	24 ± 3	619 ± 25
	st-cit	36 ± 4	109 ± 29	21 ± 4	256 ± 64	17 ± 4	676 ± 33
Eu	st[d]	70 ± 6	n. c.[e]	66 ± 5	1100 ± 39	61 ± 7	1070 ± 39
	st-cit	85 ± 9	6350 ± 164	32 ± 4	612 ± 220	25 ± 4	849 ± 32
Yb	st[d]	79 ± 4	n. c.[e]	34 ± 4	790 ± 28	27 ± 4	779 ± 18
	st-cit	89 ± 11	5370 ± 440	43 ± 2	731 ± 84	18 ± 3	689 ± 28
Zn[f]	st[d]	3 ± 1	n. d.[g]	3 ± 1	n. d.[g]	3 ± 2	n. d.[g]
	st-cit	3 ± 6	n. d.[g]	0 ± 2	n. d.[g]	0 ± 1	n. d.[g]

[a] … st = standard medium (10 % FBS without citrate), st-cit = citrate-containing st-medium (10 % FBS + 0.1 mM citrate)

[b] … values represent means ± SEM of three to eight independent experiments

[c] … values ± SEM derived from fitting of respective dose-response curves

[d] … (Heller et al., 2019)

[e] … not able to calculate

[f] … positive control

[g] … not determined

In contrast, after 8 h exposure, significant differences between both cell culture media were observed for Ce. At Ln concentrations < 10^{-5} M, the viability of NRK-52E cells is significantly enhanced compared to the untreated control in st-cit-medium. The same effect but to a lesser extent was observed for Yb. In st-medium, we also observed a slightly enhanced cell viability after Ce and Yb exposure but that was not significant. For La and Eu, dose-response curves were nearly identical in both cell culture media. Obviously, the addition of 0.1 mM citrate to the cell culture medium affects the viability of NRK-52E cells after Ln exposure during short-time exposure. Especially after 8 h exposure to Ce, the cell viability is significantly enhanced for Ln concentrations < 10^{-5} M. However, this positive effect was not observed after exposure for 24 and 48 h at all. Instead, after 48 h exposure, dose-response curves and EC_{50} values in st-cit-medium are quite similar to those in st-medium for all Ln.

The morphology of unexposed NRK-52E cells is quite identical in st-cit, st-, and sr-medium. Upon exposure with Ce the same morphological alterations like in sr-medium occur, i. e. rounding and shrinking of cells, loss of cell junctions, shrinking and loss of cytoskeleton resulting in decreased fluorescence intensity of the Phalloidin staining, and shrinking and condensation of the nucleus resulting in increased fluorescence intensity of the DAPI staining (see Figure 3).

In summary, our results demonstrate that the effect of Ln onto NRK-52E cells depends on the Ln concentration, the exposure time, and the addition of citrate to the medium. After short-time exposure of 8 h, 0.1 mM citrate addition results in significantly enhanced cell viability at Ln concentrations ≤ $5 \cdot 10^{-6}$ M, especially for Ce. In contrast, after 24 and 48 h citrate addition did not result in any significant differences in Ln cytotoxicity onto NRK-52E cells. This is in good accordance with the results reported by (Sachs et al., 2015).

Influence of citrate on the Ln speciation in cell culture medium

TRLFS studies with 10^{-5} M and 10^{-3} M Eu in st- and st-cit-medium, respectively, were performed after incubation for 24 and 48 h, respectively. Results are depicted in the ESI, Figures S8 and S9. All spectral parameters are given in the ESI, Table S3.

In general, the same spectral differences like in sr-medium are evident compared to the uncomplexed Eu aqua ion. However, in contrast to sr-medium, the luminescence decay mode was biexponential in st-cit-medium.

At constant Eu concentration, steady-state spectra and luminescence decay curves in one respective cell culture medium are quite identical after incubation for 24 and 48 h, respectively. Hence, the Eu speciation in both cell culture media remains unaltered with-

in this time frame. This proves that the effects observed in the cell culture experiments are real time effects and not caused by a different Ln speciation.

Figure 8 depicts the steady-state spectra and luminescence decay curves in dependence on citrate addition to the cell culture medium. At constant exposure time and Eu concentration, steady-state spectra and luminescence decay curves are very similar (10^{-5} M Eu) or even identical (10^{-3} M Eu) in st- and st-cit-medium, respectively. Hence, the spectral parameters derived from TRLFS studies are also very similar and the same species dominate the Eu speciation. TRLFS raw data show no significant difference between the luminescence intensity of Eu in both cell culture media (data not shown). This indicates complete solubility of Eu and fits to the solubility results.

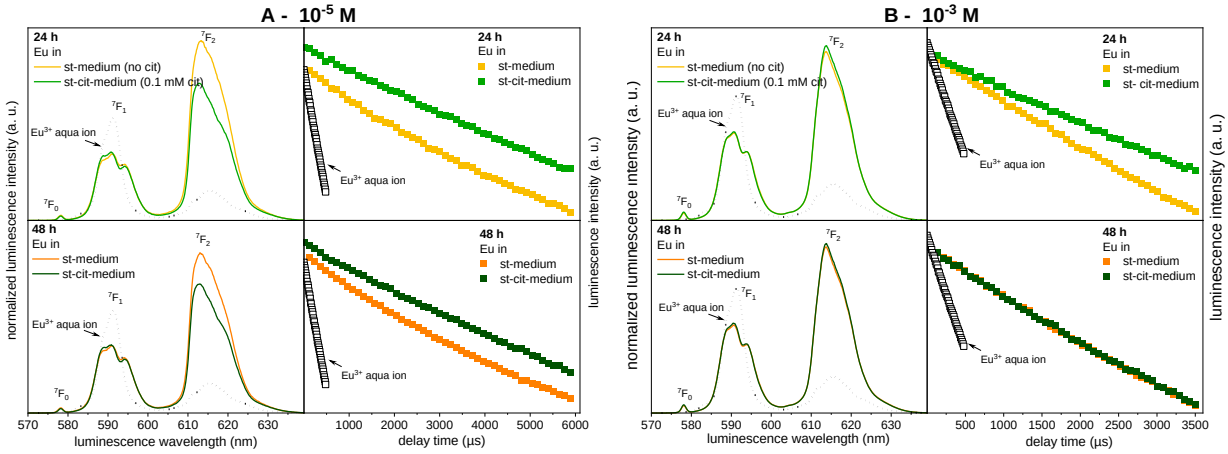

Figure 8: Comparative steady-state spectra and luminescence decay curves derived from time-resolved spectra of 10^{-5} M (A) and 10^{-3} M Eu (B) in cell culture medium with and without citrate. Data of the Eu^{3+} aqua ion are given for comparison; luminescence bands are labeled with the respective ground state of the emission transitions. The luminescence spectra and decay curves, respectively, are scaled to the same height.

Since, in st-medium, two Eu species with proteins are supposed to dominate (confer to section 3.1), we assume the same Eu complexes to form in st-cit-medium. However, since citrate is known to form stable complexes with trivalent Ln and An (Heller et al., 2011; Heller et al., 2012; Hubert et al., 1974; Itoh et al., 1985; Jackson and Dutoit, 1991; Kieboom et al., 1977), we cannot exclude the existence of a small fraction of Eu citrate

complexes which might be covered by the protein-bound Eu species in the TRLFS spectra. To study this in more detail, further measurements on Eu in sr- and sf-medium with citrate addition are already ongoing.

In summary, our TRLFS data demonstrate that Ln speciation in one respective cell culture medium does not change within the time frame of 48 h. Furthermore, TRLFS results correlate very well to those from Ln solubility studies. We suppose the same two soluble and long-lived Eu species with proteins from FBS (Eu species 1 and 2) to be formed in st- and st-cit-medium. Hence, citrate addition has no significant influence on both the solubility and the speciation of Eu in cell culture medium. With regard to the cell culture experiments, this would explain why the effect of Ln onto NRK-52E is very similar in st- and st-cit-medium after exposure for 24 and 48 h.

Thermodynamic modelling of Ln speciation in cell culture medium with citrate addition

The predicted Eu speciation in st-cit-medium at both concentrations used for TRLFS is depicted in Figure S11. At both 10^{-5} M and 10^{-3} M Eu, in the experimental pH-range of 7.6 ± 0.2, the speciation is dominated by soluble carbonate and phosphate complexes with the negatively charged dicarbonato complex being the biggest fraction by far (> 70 %). At both Eu concentrations, a fraction of 1 – 10 % is calculated to exist as citrate complexes, i. e. the 1:1- and 1:2-complex, respectively, with the threefold negatively charged citrate anion ($HCit^{3-}$). Complexes with other organic constituents are negligible. Strikingly, no Eu complexes with transferrin are predicted to form. This is clearly contrary to the results from Ln solubility and TRLFS.

Out of the two citrate species, the neutral EuHCit is predicted to be the dominant species and $Eu(HCit)_2^{3-}$ the minor species. In aqueous solutions of 30 µM Eu + 1 mM citrate, complexes with the citrate anion are reported to dominate the speciation in the same

pH-range (Heller et al., 2012). However, in aqueous solution, $Eu(HCit)_2^{3-}$ and EuHCit make up 90 and 10 % of the Eu fraction, respectively (Heller et al., 2012), whereas, in the cell culture medium, EuHCit is the bigger fraction (Figure S10). This difference is most probably due to matrix cations like calcium, magnesium, and iron concurring with the Ln for citrate complexation. Additionally, the carbonate and phosphate concentrations of DMEM exceeding that of citrate by one to two orders of magnitude (44 mM for HCO_3^- and 1 mM for $H_2PO_4^-$) might also alter the equilibrium between the Eu citrate species.

In summary, according to thermodynamic modeling, Eu speciation in st- and st-cit-medium should differ significantly. Consequently, also the TRLFS spectra and luminescence lifetimes should differ. However, our TRLFS data demonstrate that this is not the case. Hence, it can be concluded that, currently, thermodynamic modeling cannot predict the effect of citrate on the Eu speciation in cell culture medium properly.

4. Discussion

Influence of FBS on Ln solubility, cytotoxicity, and speciation

Results of our solubility studies prove that Ln solubility strongly depends on the serum content of the cell culture medium and the Ln concentration whereas it seems to be independent from incubation time (up to 48 h) and the Ln element. In st-medium, all Ln are completely soluble up to 10^{-3} M. Reducing the FBS content of the cell culture medium results in significant decrease of Ln solubility and leads to precipitation of Ln deposits with an elemental ratio of Ln : P ~ 1 : 1 at Ln concentrations above 10^{-4} M. Furthermore, differences between sf- and sr-medium demonstrate a concentration-dependent effect of FBS. We assume proteins from FBS to bind to the Ln, thus, keeping them in solution.

This might also facilitate Ln bioavailability. If the FBS concentration is too low to complex all Ln, hardly soluble complexes with inorganic constituents from DMEM, most probably phosphates, are formed and precipitate.

In general, our results are in very good accordance to literature data. (Filerman and Berliner, 1980) reported that Pb is also less soluble in serum-free cell culture medium and FBS acts to solubilize or suspend the heavy metal ions in cell culture media. The same is reported for Eu (Sachs et al., 2015). The same authors also found a ratio of Ln : P ~ 1 : 1 for Eu precipitates from DMEM, verifying our results.

Results of our cell culture experiments reveal that the cytotoxic effect of Ln onto rat renal NRK-52E cells depends on Ln concentration, exposure time, and the FBS content of the cell culture medium. In st-medium, Ln cytotoxicity seems to increase with prolonged exposure time within 8 – 48 h (Heller et al., 2019). The same holds true for sr-medium with reduced FBS content within the time frame of 24 – 48 h. However, reducing the FBS content of the cell culture medium significantly strengthens the effect of Ln onto the viability of NRK-52E cells, at least after exposure for 48 h. TRLFS results rule out different Ln species to be responsible for this effect but give hints that the soluble fraction of Eu might decrease with time and more Eu precipitates. This might be an indication that the insoluble Eu species might be responsible for the stronger effect in sr-medium. This hypothesis is further supported by our TRLFS results indicating the same Eu species with protein(s) from FBS to dominate in st-medium and the supernatant of sr-medium. Hence, if the soluble Ln species would be the effective one, the impact of Ln onto the cell viability should be similar or even weaker in sr-medium. However, with our methods we cannot determine whether a soluble or insoluble species provokes the effect of Ln onto NRK-52E cells. This should be further investigated in detail.

In literature, diverging effects of FBS on the cytotoxicity of heavy metals are reported. On the one hand, (Haase et al., 2015) demonstrated a so-called "cytoprotective effect" of FBS within studies of Zn cytotoxicity onto four different mammalian cell lines (human acute T-cell leukemia cell line Jurkat, murine macrophages RAW 264.7, murine microglial cell line BV-2, and murine fibroblasts L929). The authors explain this by FBS complexing Zn, thus maintaining a very low concentration of "free Zn", i. e. exchangeable Zn complexed by low molecular weight ligands. Hence, lowering the FBS content resulted in decreased EC_{50} values in cell culture medium with lower FBS content This effect was confirmed for Ag, Cu, Pb, Cd, Hg, and Ni within the same study. Along with increased cytotoxicity, an increased intracellular uptake of Zn (Haase et al., 2015). (Dominguez et al., 2002) also found a protective effect of FBS for Pb exposed normal human dermal fibroblasts. In contrast, (Filerman and Berliner, 1980) report a higher cytotoxicity of Pb onto an epitheliod cell line in cell culture medium with FBS than in serum-free one.

In literature, also data for U, Cd, Zn, and Cu cytotoxicity onto NRK-52E cells in sf-medium are reported (Carriere et al., 2004; Carriere et al., 2006; Milgram et al., 2007; Thiebault et al., 2007). It is questionable, whether the observed effects can be solely described to the cytotoxicity of the heavy metals. In fact, we suppose that the absence of FBS plays an essential role in the reported cytotoxic effects. Since FBS contains multiple vitamins and growth factors essential for cells, reducing or removing the serum content of a cell culture medium leads to significant cellular stress. The cell metabolism adopts trying to compensate the deficiency or lack of FBS. This may also lead to a different strength of cellular response to heavy metal exposure. Hence, the reported literature values for heavy metal toxicity in sf-medium should be handled with caution or not be taken into account.

In general, our results are in very good accordance to literature data on the cytotoxicity of Pb (Dominguez et al., 2002), Eu (Sachs et al., 2015), Zn and other divalent heavy metal ions (Haase et al., 2015) in cell culture media of different FBS content reporting a protective effect of FBS.

Influence of citrate on Ln solubility, cytotoxicity, and speciation

Results of our solubility studies prove that citrate addition to the cell culture medium does not alter the solubility of Ln, at least under standard conditions with 10 % FBS. This is in good accordance with previous investigations on Eu (Sachs et al., 2015) as well as U (Carriere et al., 2006) and might be due to the fact that in both cell culture media, the metal ions are most probably complexed by serum protein(s) (Dominguez et al., 2002; Haase et al., 2015; Heller et al., 2019; Sachs et al., 2015; Sargazi et al., 2013). However, literature data suggest that citrate might be able to partially prevent Ln precipitation under serum-free conditions (Sachs et al., 2015). Hence, it would be of interest to investigate the capability of citrate to re-solubilize Ln under serum-deficient conditions.

Results of our cell culture experiments in st-cit-medium reveal a remarkable enhancement of the cell viability after short-time exposure for 8 h at Ln concentrations below $5 \cdot 10^{-6}$ M. Hence, Ln exhibit both positive and negative effects on the viability of NRK-52E cells at low and high concentrations, respectively. This is especially evident for Ce and illustrates the biphasic trend of dose-response relationships of Ln leading to controversial discussions in literature whether Ln have beneficial or detrimental effects onto cells and living organisms (Gwenzi et al., 2018).

For short-time exposure of human foreskin fibroblasts (HFF) with Ce, an analog increase in cell viability is reported whereas this effect was not observed when using murine preosteoblastic (MC3T3-E1) cells (Schmidlin et al., 2012). For cardiac fibroblasts ex-

posed to Ce for 24 – 96 h a significant increase in cell viability is reported, too (Preeta and Nair, 1999). Furthermore, this study indicated that Ce might enhance the proliferation rate by stimulation of superoxide anion generation. Unfortunately, the authors did not state the chemical form in which Ce was applied.

An analog trend like in st-cit-medium was also observed for NRK-52E cells in st-medium after exposure to Ce for 8 h but the effect was not so strong like in st-cit-medium (Heller et al., 2019). Reasons for the enhanced cell viability at low Ln concentrations are still unclear but might be an alteration of either the proliferation or the apoptosis/necrosis of the NRK-52E cells by the Ln and/or citrate. This is subject of further investigations.

In contrast to short-time exposure, cell viabilities measured after Ln exposure for 24 and 48 h differ only slightly. This fits to solubility and TRLFS results indicating the same soluble Eu species with protein(s) from FBS to be formed in both cell culture media. In literature, diverging results are reported regarding the influence of citrate on heavy metal cytotoxicity. On the one hand, one group (Carriere et al., 2008; Carriere et al., 2006; Milgram et al., 2007) demonstrated that U is more cytotoxic to several mammalian cell lines (NRK-52E, human fibroblast cell line MG-63 derived from bone osteosarcoma, and rat osteoblast-like bone cell line ROS 17/2.8 originating from an osteosarcoma) and that intracellelular accumulation is higher when U is applied as citrate complex in comparison to U bicarbonate Furthermore, Zn is reported to be cytotoxic to pig kidney LLC-PK1 cells only when applied in citrate buffer, whereas Zn in deionized water or PBS has no significant effect (Sargazi et al., 2013). On the other hand, (Mirto et al., 1999) report a lack of U cytotoxicity onto LLC-PK1 cells when administered as citrate complex compared to the bicarbonate complex which exhibits cytotoxicity. Finally, we previously reported on the cytotoxic effect of Eu onto FaDu cells but observed no significant differences between cell culture medium with and without citrate (Sachs et al., 2015).

However, when citrate was added to sf-medium in a ratio of Ln : cit = 1 : 10, the cytotoxic effect of Eu was significantly weaker. Hence, it would be of great interest to further study the effect of citrate on Ln cytotoxicity in serum-deficient medium.

Exceptional strong effect of Ce

Results of our cell culture studies demonstrate that the effect of Ln exposure onto NRK-52E cells also depends on the respective Ln element. Concerning the toxicity gradient, a clear trend was observed independent from exposure time and cell culture medium with Ce being the only Ln significantly reducing the viability of NRK-52E cells in every single experimental series. Depending on the cell culture medium and the exposure time, the difference in effect size between Ce and the other three Ln varies and can be as large as one magnitude. Interestingly, the remarkable enhancement of cell viability after Ln exposure for 8 h in st-cit-medium was also only significant for Ce. Therefore, Ce is by far the most interesting Ln element out of these four. Moreover, we even assume Ce to be the most cytotoxic element within the whole Ln family which is in accordance with literature (Feyerabend et al., 2010; Hirano and Suzuki, 1996; Nakamura et al., 1997; Palmer et al., 1987).

Available data on the effect of other heavy metals onto NRK-52E cells after 24 h exposure is summarized in (Heller et al., 2019). Under serum-free conditions, the EC_{50} values for Cd, Zn, and Cu, the three most effective heavy metal elements, lie in the range of (0.4 – 2.6) · 10^{-4} M (Milgram et al., 2007). This is close to the EC_{50} value of 1.8 · 10^{-4} M for Ce under serum-reduced conditions determined in the present study. However, since data of (Milgram et al., 2007) were obtained in cell culture medium without any FBS while in our studies 1 % FBS was present, the EC_{50} values are not directly comparable. Neverthe-

less, it is indispensable to mention that totally different effects and mechanisms than heavy metal exposure lead to cell death upon cultivation in sf-medium.

Up to now, the reason for the exceptional strong effect of Ce is still unknown. Most likely, it is caused by its chemical characteristics. Out of the 14 Ln, Ce is the only element which might be stabilized in solution in the oxidation state +IV under certain conditions. Since Ce(IV) is highly reactive, a strong oxidizing agent, and reported to have a significantly stronger cytotoxicity onto *Chironomus ramosus* than Ce(III) (Kumar et al., 2016), the partial oxidation of Ce(III) to Ce(IV) is the most probable explanation for the significantly stronger effect of Ce compared to La, Eu, and Yb. However, proof of this hypothesis has yet to be provided and further studies on the oxidation state of Ce inside the cells or the oxidative stress after exposure to Ce and other Ln are needed.

Suitability of TRLFS and thermodynamic modeling for Ln speciation in cell culture media

Results of our TRLFS study reveal that Ln speciation in cell culture media is independent from incubation time and complex. We identified four different Eu species with at least two of them coexisting in each cell culture medium. Two soluble and long-lived complexes with (a) protein(s) from FBS dominate the Eu speciation in st- and st-cit-medium (Eu species 1 and 2). At least one of these two Eu species also dominates in the supernatant of sr-medium after settlement of the Eu precipitate. An insoluble and long-lived Eu species with one or more ligands from DMEM, most probably phosphate and/or carbonate (Eu species 3), dominates the suspensions of sr- and sf-medium with stirred Eu precipitates as well as the precipitated Eu deposits. Finally, a soluble and short-lived Eu complex with an (in-) organic ligand from DMEM dominates the speciation in the supernatant of sf-medium after settlement of the Eu precipitate. In general, the TRLFS results are in good accordance with those from solubility studies. Overall, they also fit quite well

to cell culture experiments. Concerning literature data, our results fit to previous studies on Eu in cell culture media (Heller et al., 2019; Sachs et al., 2015). Finally, TRLFS has proven to be a versatile tool to experimentally investigate the speciation of luminescent heavy metal ions in a complex solution like a cell culture medium.

However, comparison of the theoretical Eu speciation in cell culture media derived from thermodynamic modeling and TRLFS results yielded significant discrepancies. Thus, quite identical Ln speciation was predicted in st-, sr-, sf-, as well as st-cit-medium. One possible explanation might be an underestimation of the Eu complexation by transferrin, another one the existence of Eu complexes with other proteins (albumin, globulin, lipo-proteins) or even ternary Eu complexes for which no thermodynamic data are available up to now. In fact, there is an ongoing controversy whether Ln are better complexed by transferrin or albumin in biological fluids (Duffield et al., 1994; Palizban et al., 2010; Taylor, 1998). This points to the need for detailed investigations on the composition of FBS and the binding of Eu to the proteins contained therein to determine complex formation constants. With these, thermodynamic databases could be supplemented and the predicted speciation would be more reliable. Furthermore, it has to be kept in mind, that FBS is a natural product with variable content of its components. Hence, some variance has always to be accepted.

Another possible explanation for the modeling deviating from experimental results might be an insufficient thermodynamic database. For modeling, thermodynamic data for the hydrolysis of all organic, inorganic and biological fluid components as well as their interactions with the Ln and with ubiquitous matrix cations (alkali, alkaline earth, aluminum, iron, etc.) must be known and included in the calculations. Due to the many possible combinations of potentially interacting reactants, this can easily lead to some kind of "parameter explosion" which cannot be fully parameterized. Another major

problem for the modeling is the often unclear stoichiometry of large organic compounds. Smaller surrogate species without given chemical composition can be used to describe simple reactions but e. g. redox reactions involving the degradation of such species would, then, be rendered impossible.

In summary, up to now, thermodynamic modeling is hardly suitable for Ln speciation in a complex biological fluid like cell culture medium due to a huge lack of thermodynamic data. Furthermore, it has limited value for the interpretation of the TRLFS data and the assignment of Eu species. Therefore, to really identify and assign the dominant Eu species in the different cell culture media, extensive TRLFS measurements of Eu in numerous reference solutions of varying composition is indispensable. Hence, our study points to the great need of basic chemical research to render this promising method applicable for Ln speciation in biological fluids and for risk assessment.

5. Conclusions

In this study, we investigated the influence of the serum content as well as that of citrate addition onto the solubility and speciation of Ln in cell culture medium as well as on their effect on the viability of rat renal NRK-52E cells. For that, *in vitro* cell culture techniques were combined with dedicated analytical and spectroscopic methods as well as thermodynamic modeling. Experiments were performed in four different cell culture media: st-medium with 10 % FBS, sr-medium with 1 % FBS, sf-medium without any FBS, and st-cit-medium with 10 % FBS and 0.1 mM citrate addition.

In conclusion, our results illustrate the multiple parameters influencing the effect of Ln onto the viability of NRK-52E cells in different ways. Results from TRLFS and solubility measurements correlate well to those from *in vitro* cell culture experiments and this

study demonstrates the synergistic effects achieved by the combination of chemical methods and cell culture techniques. Finally, comparing the Ln concentrations with significant effects onto NRK-52E cells with those measured in unexposed waters, we conclude that, at environmental concentrations, Ln exhibit no harmful effect on rat renal cells within 8 – 48 h. Nevertheless, at elevated concentrations measured in waters of mining/industrial areas and blood samples of exposed workers, especially Ce has the potential to harmfully affect kidney cells und should be taken into account for risk assessment. However, since we studied only one respective rat kidney cell line no generalization can be made regarding tissues and species. For this, further extensive research is needed.

Conflict of interest

The authors declare no conflicts of interest.

Acknowledgements

This study was funded by the Deutsche Forschungsgemeinschaft under contract number HE 7054/2-1. Anne Heller kindly thanks Prof. Dr. Günter Vollmer from the Technische Universität Dresden, School of Science, Faculty of Biology, Institute of Zoology, Molecular Cell Physiology and Endocrinology for the possibility to conduct most part of the work in his lab group and for continuous support. Furthermore, the authors thank Sabrina Beutner from the Helmholtz-Zentrum Dresden-Rossendorf, Institute of Resource Ecology for numerous ICP-MS measurements as well as Carola Eckardt from the same institution for TOC/TIC measurements.

Appendix A. Supplementary data

Tables: Supplemented data for thermodynamic modeling of Eu and Ce speciation in cell culture medium; ICP-MS and total carbon data in sr- and sf-medium; spectral parameters derived from TRLFS spectra of Eu in cell culture media of different composition.

Figures: Dose-response curves after Ln exposure of rat NRK-52E cells in sr- and st-cit-medium; light microscopic images of Ln precipitation in 96-well-plates; dose-response curves after Ln exposure of NRK-52E cells in sr- and st-cit-medium in dependence on the exposure time; fluorescence microscopic images of NRK-52E cells exposed to Zn in sr-medium; amplified fluorescence microscopic images of NRK-52E cells in st-medium; steady-state luminescence spectra and decay curves derived from time-resolved spectra of Eu in sr-, sf-, and st-cit-medium; raw steady-state luminescence spectra of Eu in sr- and sf-medium in dependence on the incubation time; species distribution of Eu in sr- and st-cit-medium as predicted by thermodynamic modeling.

References

Abbott, T. R., 1983. Changes in Serum-Calcium Fractions and Citrate Concentrations During Massive Blood-Transfusions and Cardiopulmonary Bypass. British Journal of Anaesthesia. 55**,** 753-760.

Ansoborlo, E., et al., 2006. Actinide speciation in relation to biological processes. Biochimie. 88**,** 1605-1618.

Apostoli, P., 1999. The role of element speciation in environmental and occupational medicine. Fresenius Journal of Analytical Chemistry. 363**,** 499-504.

Aquilina, G., et al., 2016. Safety of Lancer (lanthanide citrate) as a zootechnical additive for weaned piglets. Efsa Journal. 14.

Bauer, N., et al., 2014. Interaction of Cm(III) and Am(III) with human serum transferrin studied by time-resolved laser fluorescence and EXAFS spectroscopy. Dalton Transactions. 43**,** 6689-6700.

Berthon, G., 2002. Aluminium speciation in relation to aluminium bioavailability, metabolism and toxicity. Coordination Chemistry Reviews. 228**,** PII S0010-8545(02)00021-8.

Bethke, C. M. (Ed.) 2008. Geochemical and Biogeochemical Reaction Modeling. Cambridge University Press, Cambridge.

Bladen, C. L., et al., 2013. In vitro analysis of the cytotoxic and anti-inflammatory effects of antioxidant compounds used as additives in ultra high-molecular weight polyethylene in total joint replacement components. Journal of Biomedical Materials Research Part B-Applied Biomaterials. 101B**,** 407-413.

Bresson, C., et al., 2012. The speciation in toxicology. Actualite Chimique. 26-33.

Bresson, C., et al., 2013. Analytical tools for speciation in the field of toxicology. Radiochimica Acta. 101**,** 349-357.

Bünzli, J.-C. G., 2010. Lanthanide Luminescence for Biomedical Analyses and Imaging. Chemical Reviews. 110**,** 2729-2755.

Carriere, M., et al., 2004. Influence of uranium speciation on normal rat kidney (NRK-52(E)) proximal cell cytotoxicity. Chemical Research in Toxicology. 17**,** 446-452.

Carriere, M., et al., 2005a. Cellular distribution of uranium after acute exposure of renal epithelial cells: SEM, TEM and nuclear microscopy analysis. Nuclear Instruments & Methods in Physics Research Section B-Beam Interactions with Materials and Atoms. 231**,** 268-273.

Carriere, M., et al., 2005b. Uranium(VI) complexation in cell culture medium: influence of speciation on Normal Rat Kidney (NRK-52(E)) cell accumulation. Radiochimica Acta. 93**,** 691-697.

Carriere, M., et al., 2008. Transmission electron microscopic and X-ray absorption fine structure spectroscopic investigation of U repartition and speciation after accumulation in renal cells. Journal of Biological Inorganic Chemistry. 13**,** 655-662.

Carriere, M., et al., 2006. Citrate does not change uranium chemical speciation in cell culture medium but increases its toxicity and accumulation in NRK-52E cells. Chemical Research in Toxicology. 19**,** 1637-1642.

Chen, C. Y., et al., 2001. Distribution of some rare earth elements and their binding species with proteins in human liver studied by instrumental neutron activation analysis combined with biochemical techniques. Analytica Chimica Acta. 439**,** 19-27.

Cheng, J., et al., 2012. Organic Histopathological Changes and its Function Damage in Mice Following Long-term Exposure to Lanthanides Chloride. Biological Trace Element Research . 145, 361-368.

Cuddihy, R. G., Boecker, B. B., 1970. Kinetics of Lanthanum Retention and Tissue Distribution in Beagle Dog Following Administration of (La-140)Cl3 by Inhalation, Gavage and Injection. Health Physics. 19**,** 419-+.

Cuddihy, R. G., Griffith, W. C., 1971. Tissue Distribution and Retention of Ba-140 and La-140 in Beagle Dogs after Inhalation of BaCl2-LaCl3 Aerosols. Health Physics. 21**,** 16-+.

Cuddihy, R. G., Griffith, W. C., 1972. Biological Model Describing Tissue Distribution and Whole-Body Retention of Barium and Lanthanum in Beagle Dogs after Inhalation and Gavage. Health Physics. 23**,** 621-+.

Dai, Y. C., et al., 2002. Effects of rare earth compounds on growth and apoptosis of leukemic cell lines. In Vitro Cellular & Developmental Biology-Animal. 38**,** 373-375.

Davies, D. M., 1962. Ion association. Butterworth, Washington, D.C.

De Larco, J. E., Todaro, G. J., 1978. Epithelioid and Fibroplastic Rat Kidney Cell Clones - Epidermal Growth-Factor (EGF) Receptors and Effect of Mouse Sarcoma-Virus Transformation. Journal of Cellular Physiology. 94**,** 335-342.

Dominguez, C., et al., 2002. In vitro lead-induced cell toxicity and cytoprotective activity of fetal calf serum in human fibroblasts. Molecular and Cellular Biochemistry. 237**,** 47-53.

Ducousso, R., Pasquier, C., 1974. Lung Contamination by Ce and La Evolution of Early Spontaneous Absorption as a Fuction of Initial Lung Burden. Health Physics. 26**,** 519-524.

Duffield, J. R., et al., The biochemistry of the f-elements. In: K. A. Gschneidner Jr., et al., Eds.), Handbook on the Physics and Chemistry of Rare Earths, Vol. 18: Lanthanides/Actinides: Chemistry. Elsevier Science B. V., Amsterdam, 1994, pp. 591-621.

Durbin, P. W., 1960. Metabolic characteristics within a chemical family. Health Physics. 2**,** 225-238.

Durbin, P. W., 1962. Distribution of the transuranic elements in mammals. Health Physics. 8**,** 665-671.

Durbin, P. W., Actinides in animals and man. In: L. R. Morss, et al., Eds.), The Chemistry of the Actinides and Transactinide Elements, fourth edition. Springer, New York, 2006, pp. 3339–3440.

El-Akl, P., et al., 2015. Linking the chemical speciation of cerium to its bioavailability in water for a freshwater alga. Environmental Toxicology and Chemistry. 34**,** 1711-1719.

Feng, L. X., et al., 2007. Ytterbium and trace element distribution in brain and organic tissues of offspring rats after prenatal and postnatal exposure to ytterbium. Biological Trace Element Research. 117**,** 89-104.

Feyerabend, F., et al., 2010. Evaluation of short-term effects of rare earth and other elements used in magnesium alloys on primary cells and cell lines. Acta Biomaterialia. 6**,** 1834-1842.

Filerman, B. A., Berliner, J. A., 1980. An *in vitro* Study of the Effects of Lead on an Epithelioid Cell-Line. Journal of Environmental Pathology and Toxicology. 3**,** 491-511.

Fraum, T. J., et al., 2017. Gadolinium-Based Contrast Agents: A Comprehensive Risk assessment. Journal of Magnetic Resonance Imaging. 46, 338-353.

Grubbs, F. E., 1969. Procedures for Detecting Outlying Observations in Samples. Technometrics. 11**,** 1-&.

Gwenzi, W., et al., 2018. Sources, behaviour, and environmental and human health risks of high-technology rare earth elements as emerging contaminants. Science of the Total Environment. 636**,** 299-313.

Haase, H., et al., 2015. The biochemical effects of extracellular Zn2+ and other metal ions are severely affected by their speciation in cell culture media. Metallomics. 7**,** 97-106.

Harrison, T. S., Scott, L. J., 2004. Lanthanum carbonate. Drugs. 64**,** 985-996.

Hatje, V., et al., 2016. Increases in Anthropogenic Gadolinium Anomalies and Rare Earth Element Concentrations in San Francisco Bay over a 20 Year Record. Environmental Science & Technology. 50**,** 4159-4168.

He, J., et al., 2010. Species and distribution of rare earth elements in the Baotou section of the Yellow River in China. Environmental Geochemistry and Health. 32**,** 45-58.

Heller, A., et al., 2011. Chemical speciation of trivalent actinides and lanthanides in biological fluids: The dominant in vitro binding form of curium(III) and europium(III) in human urine. Chemical Research in Toxicology. 24**,** 193-203.

Heller, A., et al., 2019. Effect of four lanthanides onto the viability of two mammalian kidney cell lines. Ecotoxicology and Environment Safety. 173**,** 469–481.

Heller, A., et al., 2012. Curium(III) citrate speciation in biological systems: An europium(III) assisted spectroscopic and quantum chemical study. Dalton Transactions. 41, 13969-13983

Hirano, S., Suzuki, K. T., 1996. Exposure, metabolism, and toxicity of rare earths and related compounds. Environmental Health Perspectives. 104, 85-95.

Höllriegl, V., et al., 2020. Measurement, model prediction and uncertainty quantification of plasma clearance of cerium citrate in humans. Radiation and Environmental Biophysics.

Höllriegl, V., et al., 2017. Biokinetic measurements and modelling of urinary excretion of cerium citrate in humans. Radiation and Environmental Biophysics. 56, 1-8.

Hu, Z. Y., et al., 2004. Physiological and biochemical effects of rare earth elements on plants and their agricultural significance: A review. Journal of Plant Nutrition. 27, 183-220.

Hubert, S., et al., 1974. Simultaneous Determination of Constant Formation of Citric Complexes of Americium, Curium, Californium, Einsteinium and Fermium. Journal of Inorganic and Nuclear Chemistry. 36, 2361-2366.

Itoh, H., et al., 1985. Stability constants of rare earth citrate complex species. Lanthanide Actinide Research. 1, 79-88.

Jackson, G. E., Dutoit, J., 1991. Gadolinium(III) In Vivo Speciation. 1. A Potentiometric and Spectroscopic Study of Gadolinium(III) Citrate Complexes. Journal of the Chemical Society-Dalton Transactions. 1463-1466.

Kakuta, K., et al., 1997. High levels of ferritin and its iron in fetal bovine serum. Comparative Biochemistry and Physiology a-Molecular & Integrative Physiology. 118, 165-169.

Khan, A. M., et al., 2017. Chemical speciation and bioavailability of rare earth elements (REEs) in the ecosystem: a review. Environmental Science and Pollution Research. 24, 22764-22789.

Kieboom, A. P. G., et al., 1977. Complexation of Acetate, Glycolate, Lactate, Malate and Citrate Anions with Lanthanide(III) Cations in Aqueous-Solution as Studied by NMR-Spectroscopy. Recueil Des Travaux Chimiques Des Pays-Bas. 96, 315-316.

Kimura, T., et al., 2001. Luminescence study on solvation of americium(III), curium(III) and several lanthanide(III) ions in nonaqueous and binary mixed solvents. Radiochimica Acta. 89, 125-130.

Kiss, T., Odani, A., 2007. Demonstration of the importance of metal ion speciation in bioactive systems. Bulletin of the Chemical Society of Japan. 80, 1691-1702.

Kubota, Y., et al., 2000. Different cytotoxic response to gadolinium between mouse and rat alveolar macrophages. Toxicology in Vitro. 14, 309-319.

Kulaksiz, S., Bau, M., 2013. Anthropogenic dissolved and colloid/nanoparticle-bound samarium, lanthanum and gadolinium in the Rhine River and the impending destruction of the natural rare earth element distribution in rivers. Liebigs Annalen - Recueil. 362, 43-50.

Kumar, A., et al., 2016. The interaction of actinide and lanthanide ions with hemoglobin and its relevance to human and environmental toxicology. Journal of Hazardous Materials. 307, 281-293.

Lawal, A. O., Ellis, E., 2010. Differential sensitivity and responsiveness of three human cell lines HepG2, 1321N1 and HEK 293 to cadmium. Journal of Toxicological Sciences. 35, 465-478.

Lee, W. K., et al., 2017. Initial autophagic protection switches to disruption of autophagic flux by lysosomal instability during cadmium stress accrual in renal NRK-52E cells. Archives of Toxicology. 91, 3225-3245.

Leggett, R., et al., 2014. Biokinetic data and models for occupational intake of lanthanoids. International Journal of Radiation Biology. 90**,** t.

Levina, A., et al., 2017. Speciation of metal drugs, supplements and toxins in media and bodily fluids controls in vitro activities. Coordination Chemistry Reviews. 352**,** 473-498.

Li, X., et al., 2007. Microcalorimetric studies on the interactions of lanthanide ions with bovine serum albumin. Journal of Thermal Analysis and Calorimetry. 89**,** 899-905.

Li, X. F., et al., 2014. Distribution and fractionation of rare earth elements in soil-water system and human blood and hair from a mining area in southwest Fujian Province, China. Environmental Earth Sciences. 72**,** 3599-3608.

Li, X. F., et al., 2013. A human health risk assessment of rare earth elements in soil and vegetables from a mining area in Fujian Province, Southeast China. Chemosphere. 93**,** 1240-1246.

Lindl, T., 2002. Zell- und Gewebekultur. Spektrum Akademischer Verlag, Heidelberg.

MacMillan, G. A., et al., 2017. Rare earth elements in freshwater, marine, and terrestrial ecosystems in the eastern Canadian Arctic. Environmental Science-Processes & Impacts. 19**,** 1336-1345.

Maulik, G., et al., 1992. Curative effect of methionine on certain enzymes of chick kidney cortex under lanthanum toxicity situation. Indian Journal of Experimental Biology. 30 (12), 1166-1169.

May, P. M., et al., JESS database. 2018.

Milgram, S., et al., 2007. Cell-metal interactions: A comparison of natural uranium to other common metals in renal cells and bone osteoblasts. Nuclear Instruments & Methods in Physics Research Section B-Beam Interactions with Materials and Atoms. 260**,** 254-258.

Mirto, H., et al., 1999. Influence of uranium(VI) speciation for the evaluation of in vitro uranium cytotoxicity on LLC-PK1 cells. Human & Experimental Toxicology. 18**,** ka180-187.

Moeller, P., et al., 2014. Seasonal variations of rare earths and yttrium distribution in the lowland Havel River, Germany, by agricultural fertilization and effluents of sewage treatment plants. Applied Geochemistry. 41**,** 62-72.

Moll, H., et al., 2014. Interactions of the Mont Terri Opalinus Clay Isolate Sporomusa sp MT-2.99 with Curium(III) and Europium(III). Geomicrobiology Journal. 31**,** 682-696.

Nakamura, Y., et al., 1997. Differences in behavior among the chlorides of seven rare earth elements administered intravenously to rats. Fundamental and Applied Toxicology. 37**,** 106-116.

Negrel, P., et al., 2000. Rare earth elements, neodymium and strontium isotopic systematics in mineral waters: evidence from the Massif Central, France. Applied Geochemistry. 15**,** 1345-1367.

Oral, R., et al., 2017. Heavy rare earth elements affect early life stages in Paracentrotus lividus and Arbacia lixula sea urchins. Environmental Research. 154**,** 240-246.

Ozaki, T., et al., 2002. Empirical method for prediction of the coordination environment of Eu(III) by time-resolved laser-induced fluorescence spectroscopy. Analytical and Bioanalytical Chemistry. 374**,** 1101-1104.

Pagano, G., et al., 2015. Rare earth elements in human and animal health: State of art and research priorities. Environmental Research. 142**,** 215-220.

Pagano, G., et al., 2016. Comparative toxicities of selected rare earth elements: Sea urchin embryogenesis and fertilization damage with redox and cytogenetic effects. Environmental Research. 147, 453-460.

Paiva, A. V., et al., 2009. Effects of Lanthanum on Human Lymphocytes Viability and DNA Strand Break. Bulletin of Environmental Contamination and Toxicology. 82, 423-427.

Palizban, A. A., et al., 2010. Effect of cerium lanthanide on Hela and MCF-7 cancer cell growth in the presence of transferrin. Research in Pharmaceutical Sciences. 5, 119-125.

Palmer, R. J., et al., 1987. Cytotoxicity of the Rare-Earth-Metals Cerium, Lanthanum, and Neodymium *in vitro* - Comparisons with Cadmium in a Pulmonary Macrophage Primary Culture System. Environmental Research. 43, 142-156.

Porru, S., et al., 2001. The potencial role of rare earths in the pathogenesis of interstitial lung disease: a case report of movie projectionist as investigated by neutron activation analysis. Journal of Trace Elements in Medicine and Biology. 14, 232-236.

Prat, O., et al., 2005. Transcriptomic and proteomic responses of human renal HEK293 cells to uranium toxicity. Proteomics. 5, 297-306.

Preeta, R., Nair, R. R., 1999. Stimulation of cardiac fibroblast proliferation by cerium: a superoxide anion-mediated response. Journal of Molecular and Cellular Cardiology. 31, 1573-1580.

Puigdomènech, I., HYDRA: Hydrochemical Equilibrium Constant Database. 2009.

Richardson, F. S., 1982. Terbium(III) and europium(III) ions as luminescent probes and stains for biomolecular systems. Chemical Reviews. 82, 541-552.

Richmond, C. R., London, J. E., 1966. Long-Term *in vivo* Retenteion of Cerium-144 by Beagles. Nature. 211, 1179-&.

Rim, K. T., et al., 2013. Toxicological evaluations of rare earths and their health impacts to workers: a literature review. Saf Health Work. 4, 12-26.

Sachs, S., et al., 2015. Interaction of Eu(III) with mammalian cells: Cytotoxicity, uptake, and speciation as a function of Eu(III) concentration and nutrient composition. Toxicology in Vitro. 29, 1555-1568.

Sargazi, M., et al., 2013. Zinc induced damage to kidney proximal tubular cells: Studies on chemical speciation leading to a mechanism of damage. Journal of Trace Elements in Medicine and Biology. 27, 242-248.

Schmidlin, P. R., et al., 2012. Effect of cerium chloride application on fibroblast and osteoblast proliferation and differentiation. Archives of Oral Biology. 57, 892-897.

Scudiero, D. A., et al., 1988. Evaluation of a Soluble Tetrazolium Formazan Assay for Cell-Growth and Drug Sensitivity in Culture Using Human and Other Tumor-Cell Lines. Cancer Research. 48, 4827-4833.

Shen, L., et al., 2010. Proteomic analysis of lanthanum citrate-induced apoptosis in human cervical carcinoma SiHa cells. Biometals. 23, 1179-1189.

Shen, L., et al., 2009a. Comparative proteomics analysis of lanthanum citrate complex-induced apoptosis in HeLa cells. Science in China Series B-Chemistry. 52, 1814-1820.

Shen, L., et al., 2009b. A proteomic investigation into the human cervical cancer cell line HeLa treated with dicitratoytterbium (III) complex. Chemico-Biological Interactions. 181, 455-462.

Spencer, A. J., et al., 1997. Gadolinium Chloride Toxicity in the Rat. Toxicologic Pathology. 25 (3), 245-255.

Su, X. G., et al., 2009. Lanthanum citrate induces anoikis of Hela cells. Cancer Letters. 285**,** 200-209.
Taylor, D. M., 1998. The bioinorganic chemistry of actinides in blood. Journal of Alloys and Compounds. 271**,** 6-10.
Tepe, N., et al., 2014. High-technology metals as emerging contaminants: Strong increase of anthropogenic gadolinium levels in tap water of Berlin, Germany, from 2009 to 2012. Applied Geochemistry. 45**,** 191-197.
Thiebault, C., et al., 2007. Uranium induces apoptosis and is genotoxic to normal rat kidney (NRK-52(E)) proximal cells. Toxicological Sciences. 98**,** 479-487.
Trifuoggi, M., et al., 2017. Comparative toxicity of seven rare earth elements in sea urchin early life stages. Environmental Science and Pollution Research. 24**,** 20803-20810.
Vergauwen, E., et al., 2018. Central nervous system gadolinium accumulation in patients undergoing periodical contrast MRI screening for hereditary tumor syndromes. Hereditary Cancer in Clinical Practice. 16.
Wells, H. W., Wells, V. L., The Lanthanides, Rare Earth Elements. Patty's Toxicology, Sixth Edition. John Wiley & Sons, Inc., 2012.
Yu, L., et al., 2007. Effects of rare earth elements on telomerase activity and apoptosis of human peripheral blood mononuclear cells. Biological Trace Element Research. 116**,** 53-59.
Yu, S. W., et al., 2005. La3+-Promoted proliferation is interconnected with apoptosis in NIH 3T3 cells. Journal of Cellular Biochemistry. 94**,** 508-519.
Zhang, H., et al., 2000. Rare-earth element distribution characteristics of biological chains in rare-earth element-high background regions and their implications. Biological Trace Element Research. 73**,** 19-27.
Zhang, Y., et al., 2009. Gadolinium promoted proliferation and enhanced survival in human cervical carcinoma cells. Biometals. 22**,** 511-519.
Zhao, H., et al., 2013. Oxidative stress in the kidney injury of mice following exposure to lanthanides trichloride. Chemosphere. 93**,** 875-884.
Zhu, W. F., et al., 1996. Investigation on the intelligence quotient of children in the areas with high REE background .1. REE bioeffects in the REE-high areas of southern Jiangxi Province. Chinese Science Bulletin. 41**,** 1977-1981.